Key Words:
Saltstone Disposal Facility,
Radon, Airborne Pathway,
Performance Assessment

Retention: Permanent

AIR AND RADON PATHWAY MODELING FOR THE SALTSTONE DISPOSAL FACILITY

Kenneth Dixon
Greg Flach
Miles Denham
Mark Phifer

DECEMBER 2008

Savannah River National Laboratory
Savannah River Nuclear Solutions
Aiken, SC 29808

Prepared for the U.S. Department of Energy Under
Contract Number DE-AC09-08SR22470

SRNL

DISCLAIMER

Printed in the United States of America

Prepared For
U.S. Department of Energy

Key Words:
Saltstone Disposal Facility,
Radon, Airborne Pathway,
Performance Assessment

Retention: Permanent

AIR AND RADON PATHWAY MODELING FOR THE SALTSTONE DISPOSAL FACILITY

DECEMBER 2008

Savannah River National Laboratory
Savannah River Nuclear Solutions
Aiken, SC 29808

Prepared for the U.S. Department of Energy Under
Contract Number DE-AC09-08SR22470

SRNL

REVIEWS AND APPROVALS

Authors

Kenneth Dixon, Environmental Sciences and Biotechnology — Date: 12/17/2008

Greg Flach, Environmental Sciences and Biotechnology — Date: 12/17/2008

Miles Denham, Environmental Sciences and Biotechnology — Date: 12/17/2008

Mark Phifer, Environmental Sciences and Biotechnology — Date: 12/17/08

Design Check

Tad Whiteside, Environmental Sciences and Biotechnology — Date: 12/17/08

Approvals

Jack Mayer, Manager, Environmental Sciences and Biotechnology — Date: 12/17/2008

Bob Aylward, Manager, Environmental Sciences and Biotechnology — Date: 12/17/08

Heather Burns 12/18/2008

Heather Burns, Project Manager, Environmental and Chemical Processing Technology Date

David A. Crowley 12/18/08

Dave Crowley, Manager, Radiological Performance Assessment Date

Sharon F Marra 12/22/08

Sharon Marra, Manager, Environmental and Chemical Processing Technology Date

Marcia Birk 1/6/09

Marcia Birk, 3116 Documentation Preparation Date

Kent H. Rosenberger 1/6/09

Kent Rosenberger, Lead, 3116 Documentation Preparation Date

TABLE OF CONTENTS

LIST OF FIGURES

LIST OF TABLES

LIST OF ACRONYMS

ARP	Actinide Removal Process
Ci	Curie
CSSX	Caustic side solvent extraction
DDA	Deliquification, Dissolution, and Adjustment
DRF	Dose Release Factor
ETF	Effluent Treatment Facility
ITP	In-Tank Precipitation Facility
K_s	Saturated Hydraulic Conductivity
LLW	Low Level Waste
MCU	Modular Caustic Side Solvent Extraction Unit
MEI	Maximally Exposed Individual
NRC	Nuclear Regulatory Commission
PA	Performance Assessment
pCi	picoCurie
SDF	Saltstone Disposal Facility
SRNL	Savannah River National Laboratory
SRS	Savannah River Site
SWPF	Salt Waste Processing Facility
USDOE	United States Department of Energy
w/pm	Water to premix
WMAP	Waste Management Area Projects
WRA	Water reducing admixture

1.0 EXECUTIVE SUMMARY

SRS is currently in the process of revising the Performance Assessment (PA) for the SDF as required by DOE Order 435.1, Radioactive Waste Management. As part of the PA process, an analysis was conducted to evaluate the potential magnitude of gaseous release of radionuclides from the SDF over the 10,000-year post-closure compliance period. Specifically, an air and radon pathways analysis has been conducted to estimate the flux of volatile radionuclides and radon at the ground surface due to waste stored in Vault 1, Vault 2, and Vault 4 following closure. This analysis was used as the basis to estimate the dose to the maximally exposed individual (MEI) for the air pathway per Curie (Ci) of each radionuclide in each disposal unit.

For the air pathway analysis, several gaseous radionuclides were considered. These included carbon-14 (C-14), chlorine-36 (Cl-36), iodine-129 (I-129), selenium-79 (Se-79), antimony-125 (Sb-125), tin-126 (Sn-126), tritium (H-3), and technetium-99 (Tc-99). The dose to the MEI per Ci disposed was estimated at the SRS Boundary and at the 100 m compliance point.

For the radon pathway analysis, five parent radionuclides and their progeny were analyzed. These parent radionuclides included uranium-238 (U-238), plutonium-238 (Pu-238), uranium-234 (U-234), thorium-230 (Th-230), and radium-226 (Ra-226). The peak flux of radon-222 due to each parent radionuclide was estimated for the compliance period of 10,000 years.

2.0 INTRODUCTION

The Saltstone Disposal Facility (SDF), located in the Z-Area of the Savannah River Site (SRS), is used for the disposal of low-level radioactive salt solution. The SDF currently contains two disposal units: Vault 1 and Vault 4. Additional disposal cells are currently in the design phase. Vault 4 is approximately 200 feet wide, 600 feet in length, and 26 feet in height. Vault 4 is divided into 12 cells with each cell measuring about 100 feet by 100 feet (Phifer et al., 2006). Vault 1 is half the size of Vault 4 measuring approximately 100 feet wide by 600 feet long with 6 cells. Vault 2 is currently in the design phase. The individual cells of the saltstone facility may be filled with saltstone or in some cases other low-level radioactive waste encapsulated in grout. Saltstone is produced by mixing low-level radioactive salt solution, with blast furnace slag, fly ash, and cement to form a dense, micro-porous, monolithic, low-level radioactive waste form. The saltstone material contains no coarse or fine aggregate and is pumped into the disposal cells where it subsequently solidifies. Figure 1 provides the general location of the SDF and the surrounding topography whereas Figure 2 provides an aerial view of the facility.

For this analysis, three formulations of saltstone are considered: 1) Deliquification, Dissolution, and Adjustment (DDA) salt simulant (w/pm 0.60), 2) Actinide Removal Process (ARP)/ Modular Caustic Side Solvent Extraction Unit (MCU) salt simulant (w/pm 0.60), and 3) Salt Waste Processing Facility (SWPF) salt simulant (w/pm 0.60).

Phifer et al. (2006) gives the status of disposals in Vaults 1 and Vault 4. Vault 1 consists of six cells of which three are empty. The remaining three cells are filled with saltstone made with In-Tank Precipitation (ITP) process wastewater and Effluent Treatment Facility (ETF) wastewater concentrate. It is assumed in this analysis that saltstone made with DDA and ARP/MCU simulant is representative of the wastes contained in Vault 1. Vault 4 consists of twelve cells. One cell in Vault 4 is filled with 10,000 55-gallon drums of Naval Fuels waste encapsulated in grout. Three cells are either partially or completely filled with saltstone made with either Tank 49 solids or ETF wastewater. Five cells have been partially filled with DDA saltstone. The remaining cells will be filled with either DDA or ARP/MCU saltstone. It is assumed in this analysis that saltstone made with DDA and ARP/MCU simulant is representative of the wastes contained in Vault 4. Vault 2, which is still in the design phase, and future disposal units will be primarily filled with SWPF saltstone.

SRS is currently in the process of revising the Performance Assessment (PA) for the SDF as required by DOE Order 435.1, Radioactive Waste Management. As part of the PA process, an analysis was conducted to evaluate the potential magnitude of gaseous release of radionuclides from the SDF over the 10,000-year post-closure compliance period. Specifically, an air and radon pathways analysis has been conducted to estimate the flux of volatile radionuclides and radon at the ground surface due to waste stored in Vault 1, Vault 4, and future disposal units following closure. This analysis was used as the basis to estimate the dose to the maximally exposed individual (MEI) for the air pathway per Curie (Ci) of each radionuclide in each disposal unit. The sections that follow discuss the conceptual model for the air and radon pathways analysis, the numerical implementation of the conceptual model, and the dose calculations for the MEI based on the results of the modeling.

3.0 SDF AIR AND RADON PATHWAY ANALYSIS

This section describes the details associated with computing the dose to the MEI due to radioactive disposals in the SDF. The simulation period for the air and radon pathway was 10,000 years and covered only the time period following closure cap installation. The following cases were simulated:

- Vault 1 with DDA saltstone as the representative waste
- Vault 1 with ARP/MCU saltstone as the representative waste
- Vault 2 with SWPF saltstone as the representative waste
- Vault 4 with DDA saltstone as the representative waste
- Vault 4 with ARP/MCU saltstone as the representative waste

The method employed and the key aspects of the analysis performed are discussed in the sections that follow. For the radon pathway, the peak flux at the ground surface of Rn-222 was calculated for five parent radionuclides for each disposal unit and waste configuration. The dose to the MEI was also calculated for eight radionuclides based on the gaseous flux of each at the land surface for each disposal unit and waste configuration.

The method chosen is a hybrid approach where most parameters were set to their best estimate values (i.e., based on available site-specific measurements or engineering judgment), while other parameters were set to conservative/bounding values. The conceptual PORFLOW transport model used for the air and radon pathway analysis has imbedded within it biases that are intended to be conservative where possible. The conceptual model for both the air and radon pathway analysis is the same and the PORFLOW transport model used for both pathways utilizes the same input files. Section 3.1 and its associated subsections discuss the conceptual model for the air and radon pathway analysis. Sections 3.2 and 3.3 discuss the details specific to each analysis.

3.1 AIR AND RADON PATHWAY CONCEPTUAL MODEL

The approach taken focuses primarily on a baseline scenario where nominal settings for many of the input parameters have been conservatively chosen. The main analysis tool employed is the PORFLOW code which simulates the transport of radionuclide chains (i.e., parents and daughters) in porous media. The flux of radioactive gasses at the land surface above the disposal units was evaluated for the closure configuration given by Jones and Phifer (2008). Gaseous radionuclides within the waste zone diffuse outward into the air-filled pore space of the overlying materials. Ultimately, some of the radionuclides emanate at the land surface. As such, air is the medium through which they diffuse. It is assumed that fluctuations in atmospheric pressure at the land surface that could induce small pulses of air movement into and out of the shallow soil profile over relatively short periods of time will have a zero net effect when averaged over longer time periods. Thus, advective transport of radionuclides in air-filled soil pores is not considered to be a significant process when compared to the rate of air diffusion.

The closure cap as described by Jones and Phifer (2008) consists of a top soil layer, an upper backfill layer, an erosion barrier layer, a geotextile fabric, middle backfill layer, a geotextile

fabric, upper lateral drainage layer, a geotextile fabric, a high density polyethylene (HDPE) geomembrane, a geosynthetic clay liner (GCL), a foundation layer (backfill with bentonite admix), a lower backfill layer, a geotextile filter fabric, and a lower drainage layer. The geotextile fabrics, the HDPE geomembrane, and the GCL are excluded from this analysis. By excluding these materials, the analysis will be more conservative as these materials would be expected to significantly reduce gaseous flux at the land surface (not including the geotextile fabrics). The HDPE geomembrane would have very low gaseous diffusion coefficients and the GCL would have very little air-filled porosity, since it would be at or near saturation. The top soil layer and the upper backfill layer are also excluded from the baseline analysis, since they are located above the erosion barrier and are therefore subject to erosion. For the purposes of this analysis, it is assumed that those components situated below the top of the erosion barrier remain intact for the duration of the simulation (10,000 years).

Three disposal unit designs were considered in this analysis, Vault 1, Vault 2 (i.e. future disposal unit design), and Vault 4. Schematics of the models for the three designs, including the closure cap materials, are given in Figure 3, Figure 4, and Figure 5. As mentioned previously, Vaults 1 and 4 are assumed to contain either DDA or ARP/MCU saltstone. It is assumed that future disposal units will be filled primarily with SWPF saltstone.

3.1.1 Air and Radon Pathway Diffusive Transport Model

A one-dimensional PORFLOW based diffusive transport model was created for each disposal unit. PC-based PORFLOW Version 6.10.3 was used to conduct the simulations (ACRI, 2004). PORFLOW has been widely used at the SRS and in the USDOE complex to address major issues related to groundwater and nuclear waste management.

The governing equation for mass transport of species *k* in the fluid phase is given by

$$\frac{\partial C_k}{\partial t} + \frac{\partial}{\partial x_i}\left(\frac{V_i}{R_f} C_k\right) = \frac{\partial}{\partial x_i}\left(\frac{D_{ij}}{R_f}\frac{\partial C_k}{\partial x_j}\right) + \gamma_k \qquad (1)$$

Where:

C_k	concentration of species *k*, Ci/m^3
V_i	fluid velocity in the ith direction, m/yr
D_{ij}	molecular diffusion coefficient for the species, m^2/yr
R_f	retardation factor
γ_k	net decay of species *k*, Ci/m^3 yr
i, j	direction index
t	time, yr
x	distance coordinate, m

This equation is solved within PORFLOW to evaluate transient radionuclide transport above the disposal units and to estimate gaseous radionuclide flux at the land surface over time. For this analysis, the advection term was disabled within PORFLOW and only the diffusive and net decay terms were evaluated.

The boundary conditions imposed on the entire model domain included:

- No-flux specified for all radionuclides along sides and bottom
  ($\partial C/\partial X = 0$ at x=0, x=1 and $\partial C/\partial Y = 0$ at y=0)
- Species concentration set to 0 at land surface (top of erosion barrier)
  ($C = 0$ at $y=y_{max}$)

These boundary conditions force all of the gaseous radionuclides to move upward from the waste disposal zone to the land surface. In reality, some lateral and downward diffusion occurs in the air-filled pores surrounding the waste zone; hence, ignoring this lateral and downward movement has the effect of increasing the flux at the land surface. This should introduce some conservatism in the calculated results. Simulations were conducted in transient mode for diffusive transport in air, with results being obtained over 10,000 years.

The initial condition imposed on the domain, except for the waste zone, included:

- Species concentration set to 0 at time = 0
  ($C=0$ for $0 \leq x \leq 1$ at t=0 and $C=0$ for $0 \leq y \leq y_{max}$ at t=0)

For the air pathway analysis, the initial conditions for the model assumed a 1 Ci inventory of each radionuclide uniformly spread over the waste zone. For the radon pathway analysis, an emanation factor of 0.25 was applied resulting in an initial inventory of 0.25 Ci for each parent radionuclide uniformly spread over the waste zone. This is discussed in more detail in Section 3.3.

3.1.1.1 Grid Construction

The model grid for Vault 1 and overlying cover materials was constructed as a node mesh 3 nodes wide by 58 nodes high. This mesh creates a vertical stack of 56 model elements. Figure 3 shows a schematic of the PORFLOW model grid. The model grid for Vault 2 and future disposal units and overlying cover materials was constructed as a node mesh 3 nodes wide by 64 nodes high. This mesh creates a vertical stack of 62 model elements. Figure 4 shows a schematic of the PORFLOW model grid. The model grid for Vault 4 and overlying cover materials was constructed as a node mesh 3 nodes wide by 68 nodes high. This mesh creates a vertical stack of 66 model elements. Figure 5 shows a schematic of the PORFLOW model grid. In each case, the model grid extends upward to the top of the erosion barrier, since this is the minimum possible cover thickness that could exist during the simulation period. A set of consistent units was employed in the simulations for length, mass and time, these being meters, grams and years, respectively.

3.1.1.2 Material Zone Properties and Other Input Parameters

Material properties utilized within the 1-D numerical model for each disposal unit were specified for 9 material zones defined within the model domain. The vertical layer sequence and

associated thickness for each disposal unit is given in Table 1, Table 2, and Table 3. Each material zone was assigned values of particle density, total porosity, average saturation, air-filled porosity, and air density. An effective air-diffusion coefficient was used for each radionuclide and material layer. Therefore, tortuosity was assigned a unit value in each material zone. An air fluid density of 1.24×10^3 g/m^3 at standard atmospheric conditions was used in the transport simulations (Bolz and Tuve., 1973).

Material properties for the saltstone (DDA, ARP/MCU, and SWPF) and vault concretes were taken from Dixon et al. (2008) and are given in Tables 4, 5, and 6. Material properties for the closure cap components are also presented and were taken from Jones and Phifer (2008). Average saturation values for the saltstone, grout cap, and concrete roof were taken from the SDF PA vadose zone model. Additionally, the grout cap was assumed to have the same material properties as saltstone. The air-filled porosity of the saltstone, grout cap, and concrete roof was calculated from the total porosity and average saturation.

Jones and Phifer (2008) evaluated infiltration through the closure cap materials over time as the closure cap degraded using the HELP model. Values for total porosity and volumetric moisture content for the closure cap materials and foundation layers were taken from this analysis. These values were used to calculate the average saturation and the air-filled porosity for the closure cap materials. The maximum air-filled porosity for each material layer over the 10,000-year simulation was utilized since this represented the greatest air filled porosity in which a gas could diffuse.

Table 4, Table 5, and Table 6 provide the values of particle density, total porosity, average saturation, and air-filled porosity utilized for all the layers used for each case simulated.

3.1.2 Summary of Key Air and Radon Pathway Assumptions

The following are the key air and radon pathway analysis assumptions associated with each disposal unit simulation:

- The waste in Vault 1 can be conservatively represented by either DDA or ARP/MCU saltstone.
- The waste to be placed in future disposal units can be conservatively represented by SWPF saltstone.
- The waste in Vault 4 can be conservatively represented by either DDA or ARP/MCU saltstone.
- The clean grout cap for each disposal unit has the same material properties as saltstone.
- Exclusion of the top soil, upper backfill, HDPE geomembrane, and geosynthetic clay liner make the model more conservative.
- Exclusion of all geotextile fabrics has no impact on the model.
- The final closure cap is assumed to remain physically stable below the top of the erosion barrier for the duration of the simulation (10,000 years).

3.1.2.1 Measures Implemented to Ensure Conservative Results

In this analysis, several conditions introduce conservatism into the calculations. These include:

- The use of boundary conditions that force all of the gaseous radionuclides to move upward from the waste disposal zone to the land surface. In reality, some of the gaseous radionuclides diffuse sideways and downward in the air-filled pores surrounding the waste zone, hence ignoring this has the effect of increasing the flux at the land surface.
- Not taking credit for the removal of radionuclides by pore water moving vertically downward through the model domain. This mechanism would likely remove some dissolved radionuclides, and therefore its omission has the effect of increasing the estimate of instantaneous radionuclide flux at the land surface in simulations conducted as a part of this investigation.
- Exclusion of the HDPE geomembrane and the geosynthetic clay liner. Inclusion of these materials in the model would significantly reduce the gaseous flux at the land surface due to their material properties (i.e., low air-filled porosity and/or low effective gaseous diffusion coefficient).
- Exclusion of the cover materials above the erosion barrier (i.e., top soil and upper backfill layers). Excluding these materials shortens the diffusion pathway and could increase the flux at the land surface.
- Use of the minimum closure cap thickness in the model.

3.2 SDF AIR PATHWAY MODEL

A screening analysis was conducted to determine the radionuclides of interest for the air pathway analysis (WSRC, 2008). These radionuclides included carbon-14 (C-14), chlorine-36 (Cl-36), iodine-129 (I-129), selenium-79 (Se-79), antimony-125 (Sb-125), tin-126 (Sn-126), and tritium (H-3). Subsequent to the screening analysis, technetium-99 (Tc-99) was added to the list of radionuclides of interest. A summary of the radionuclides and compounds of interest is presented in Table 7.

3.2.1 Source Term Development

The source term for the simulations was assumed to be 1 Ci of each radionuclide which was distributed uniformly throughout the liquid filled porosity of the saltstone material layer. The radionuclides were then allowed to partition between the pore fluid and the air filled porosity. Partitioning co-efficients equivalent to apparent Henry's Law constants were estimated using The Geochemist's Workbench® (Bethke, 2005). Henry's Law for solutions is:

$$m_i = f_i H$$

where m_i is the molality (moles/kilogram) of constituent i in the aqueous phase, f_i is the fugacity of constituent i in the gas phase, and H is the Henry's Law constant. Both the solution and the gas phase were assumed to behave ideally. This makes the fugacity of a constituent equal to the partial pressure of that constituent in the gas phase. Thus, the units of the Henry's Law constant are:

$$\frac{moles}{atm. \times kg}$$

Here, these are considered apparent Henry's Law constants because most of these gases dissociate in solution to species other than the aqueous species of the gas. For example, CO_2 gas dissolved in water at a pH of 11 exists primarily as the carbonate ion CO_3^-.

The gases considered for each radionuclide, their reactions with their aqueous component, and the equilibrium constants for these reactions are shown in Table 8. In all cases the fugacity of one gas for each element was higher by several orders of magnitude than the fugacity of the other gases. The highest fugacity was chosen for the estimate of the apparent Henry's Law constant for a radionuclide.

The assumptions used in the calculations are documented in Table 9. The Eh and pH values are from estimations made in Denham (2008) for moderately aged saltstone pore water conditions. The Henry's Law constants for most of the gases vary considerably with these parameters, though differently for each gas. The ionic strength of the solution was fixed at 0.015 molal primarily by Na^+ and Cl^-, to be in the range of the extended Debye-Hückel method of calculating activity coefficients used by The Geochemist's Workbench®. Nitrate is the dominant anion in the saltstone feed solution, but at equilibrium under the reducing conditions of saltstone, nitrogen exists primarily as dissolved nitrogen gas that does not contribute to ionic strength. Hence, chloride was used to balance the sodium. The initial concentrations of the radionuclides does not matter because the apparent Henry's Law constant is the ratio of the gas fugacity to the aqueous radionuclide concentration. The ratio remains constant regardless of the total concentration of the radionuclide.

Table 10 shows the results of the apparent Henry's Law constant estimations for partitioning the radionuclides of interest between pore water and the gas phase. Most of the apparent Henry's Law constants are so high as to be essentially meaningless – all of the radionuclide can be assumed to be in the aqueous phase. The exceptions are tritium, C-14, and perhaps Se-79. The reason that elements that are often considered to be relatively volatile have such low apparent Henry's Law constants is that saltstone conditions are antithetical to formation of gases from these elements. For example, at a pH of 5 the apparent Henry's Law constants of the radionuclides other than Tc-99 would be much lower. Likewise, the apparent Henry's Law constant for Tc-99 would be much lower if saltstone were at oxidizing conditions.

The primary uncertainty in these calculations is the use of lower ionic strengths in the calculations than those estimated for saltstone pore fluids. The ionic strength of the pore fluids in fresh saltstone would be on the order of 6 molal, far higher than the 0.015 molal used here. This would lead to underestimation of the amount of a radionuclide in the gas phase for all constituents except tritium. For tritium, higher ionic strength lowers the vapor pressure of water at a given temperature, thus lowering the amount of tritium in the vapor phase. For other constituents, the high ionic strengths would result in higher activity coefficients than those at lower ionic strengths. This would cause a higher degree of partitioning of the radionuclide into the gaseous phase, sometimes referred to as the "salting out" effect. However, it is unlikely that

the activity coefficients would increase by more than a factor of 10 (Nordstrom and Munoz, 1985). Such an increase would not significantly affect conclusions based on this analysis, particularly for Cl-36, I-129, Tc-99, Sn-126, Sb-125, or Sb-126. To account for the high ionic strength saltstone pore fluids would require more sophisticated solution models and it is uncertain that reliable parameters required to run these models even exist for several of the radionuclides of interest.

3.2.2 Implementation of Partitioning Coefficients in PORFLOW

PORFLOW has the capability of partitioning radionuclides between the solid and liquid phases through a distribution coefficient. However, PORFLOW does not directly have the capability of partitioning radionuclides between the liquid and gas phases through Henry's law. Therefore, in order to use PORFLOW to represent the transport of radionuclides through the gas phase while considering liquid-gas partitioning, Henry's Law constants must be converted to equivalent distribution coefficients. This section outlines the method used to make the conversion.

The apparent Henry's Law constants developed in Section 3.2.1 for each radionuclide were converted into pseudo-partitioning coefficients for use in PORFLOW. The conventional application of partitioning in PORFLOW involves the transfer of contaminant from solid to liquid phase via a linear and completely reversible reaction. This reaction is represented in the form of a distribution coefficient (K_d) which is used in the calculation of the retardation factor (Equation 1, R_f). K_d is defined as the concentration of contaminant in the solid phase relative to the concentration of contaminant in solution with typical units of ml/g (Freeze and Cherry, 1979). For the air pathway analysis, the partitioning of contaminants is from the liquid to the gas phase rather than from the solid to the liquid phase. Therefore, it was necessary to develop a relationship between the apparent Henry's Law constants and the K_d concept used in PORFLOW. The development of this relationship is presented in Appendix A and the resulting partitioning coefficients used in the PORFLOW air pathway analysis are given in Table 11.

To correctly implement the partitioning coefficients in PORFLOW, it was necessary to redefine the material properties for the saltstone layer. The typical simulation in PORFLOW involves a solid, liquid, and a gas, with partitioning of contaminants between the solid and liquid phase (via K_d) and advective and diffusive transport occurring through the liquid phase. Inputs include the bulk density of the solid phase and the porosity of the gas-liquid phase. For gaseous diffusion problems, the particle density is that of the solid material, the porosity is the void space occupied by the gas (air-filled porosity), and the fluid density is the density of air. If the gaseous contaminants are assumed to be totally in the gas phase and the waste is assumed to be dry, then the air filled porosity equals the total porosity and there is no partitioning. For this analysis, the waste was assumed to be mostly saturated with the radionuclides of interest partitioned between the gas and liquid phase. In order to implement the K_d approach to partitioning, the liquid takes on the role usually played by the solid in a typical groundwater transport problem. Likewise, the gas takes on the role usually played by the liquid. The solid phase can be thought of as having the role typically played by gas where it is not involved in the transport process. In this implementation, the total porosity is the content of the solid and gas phases. The air-filled

porosity, which is the porosity used in the transport analysis, is determined by multiplying the total porosity by the gas saturation.

Air is the fluid through which the radioactive gasses diffuse to the ground surface. As such, the fluid density input to PORFLOW was the density of air. For each simulation, a 1 Ci inventory of each radionuclide was placed in the saltstone layer and partitioned between the liquid and gas phases according to the partitioning coefficients presented in. Once in the gas phase, the radionuclides diffused to the land surface based on the diffusion coefficients presented in Table 12, Table 13, and Table 14 and the transport equation provided by equation 1.

3.2.3 Effective Air Diffusion Coefficients

The effective air diffusion coefficient of each radionuclide or compound within each material zone was determined. Nielson et al. (1984) established a relationship between moisture saturation and the radon effective air-diffusion coefficient for various pore sizes of earthen materials. Using this method, a radon effective air-diffusion coefficient was determined for each material type based upon the average moisture saturation for the material. Subsequently, using Graham's Law, the effective air-diffusion coefficient of each radionuclide or compound evaluated was determined for each material type based on the radon effective air-diffusion coefficient using the following relationship:

$$D = D'\sqrt{\frac{MWT'}{MWT}}$$

where:

D = the effective diffusion coefficient of the radionuclide of interest (m^2/yr) within the material zone of interest
D' = the effective diffusion coefficient of Rn-222 (m^2/yr) within the material zone of interest
MWT' = the molecular weight of the reference radionuclide (Rn-222)
MWT = the molecular weight of the element or compound of interest

A summary of the radon effective air-diffusion coefficients and the calculated effective air-diffusion coefficients for each radionuclide/compound by material zone are presented in Table 12, Table 13, and Table 14.

3.2.4 Air Pathway Model Results

3.2.4.1 Air Pathway Flux to Ground Surface

Model simulations were conducted to evaluate the peak flux of each radionuclide emanating from the top of the model domain. A unit inventory of 1 Ci was assigned to the waste zone for each case simulated for each radionuclide considered in the analysis. Results were output in Ci/m^2/yr per Ci/m^2, consistent with the set of units employed in the model, and are presented for

each radionuclide in Figure 6 through Figure 10. The material properties remained constant for each case for the simulation period. Hence, the transient gaseous flux at the land surface for each radionuclide is a function of radioactive decay. This is illustrated in Figure 6 through Figure 10 where each radionuclide reaches the peak emission rate and subsequently declines as a function of decay.

The peak fluxes emanating at the land surface and the time to peak flux are presented for each case simulated in Table 15 through Table 24. The results are reported in this way to facilitate calculation of human exposure at the SRS boundary and the 100 m boundary for each case simulated.

3.2.5 Air Pathway Dose Calculations

An evaluation was conducted to assess the potential dose to a maximally exposed individual (MEI) located at the SRS boundary and the 100 m location (Lee and Foley, 2008). Dose to the MEI was calculated for both the SRS boundary and the 100 m boundary for each case simulated using the peak flux for the 10,000 year simulation period. Dose-release factors (DRF) were calculated for each radionuclide potentially released from the SDF using CAP88, the EPA model for National Emissions Standards for Hazardous Air Pollutants (NESHAP). DRFs represent the dose to the receptor exposed to 1 Ci of the specified radionuclide potentially released to the atmosphere. For the receptor located at the SRS boundary, the distance from the SDF is sufficient for an assumption of a point source. However, the DRFs for the 100 m receptor requires evaluation of an area source because of the close proximity of the SDF to the 100 m receptor. For radionuclides not contained within the CAP88 library (Se-79, Cl-36), atmospheric transport was estimated by assigning surrogates with similar radiological properties (Lee and Foley, 2008). Doses for these radionuclides were estimated by applying their dosimetric properties to the surrogate's relative air concentrations estimated by the model.

Specific SRS Boundary DRFs, 100 m boundary DRFs, and the calculated exposure levels for the simulation period at the SRS boundary and 100 m boundary are presented in Table 15 through Table 24. See Lee and Foley (2008) for details on the estimation of all DRFs.

3.3 SDF RADON ANALYSIS

This section describes the investigation conducted to evaluate the potential magnitude of radon release from Vault 1, Vault 4, and future disposal units during the 10,000-year simulation period. This investigation addresses only Rn-222. It is assumed that the short half-life of Rn-220 (55.6 seconds) renders it unable to escape the disposal units and migrate to the land surface via air diffusion before it is transformed by radioactive decay.

The potential parent radionuclides that can contribute to the creation of Rn-222 are illustrated in Figure 11. The diagram indicates the specific decay chains that lead to the formation of Rn-222, as well as the half-lives for each radionuclide. The extremely long half-life of U-238 (4.468E+9 years) cause the other radionuclides higher up on the chain of parents to be of little concern with regard to their potential to contribute significantly to the Rn-222 flux at the land surface over the period of interest. In Figure 11, the parent radionuclides that were individually evaluated are

indicated with the gray shaded area (i.e., beginning with Pu-238 and U-238). Rn-222 generated within the waste zone is in the gaseous phase and diffuses outward from this zone into the air-filled soil pores surrounding the disposal units, eventually resulting in some of the radon emanating at the land surface. As such, air is the fluid through which Rn-222 diffuses, although some Rn-222 may dissolve in residual pore water.

The parent radionuclides are assumed to exist in the solid phase and therefore do not migrate upward through the air-filled pore space, although they could be leached and transported downward from the waste zone by pore water movement. This potential downward migration of the parent radionuclides was not considered in the radon analysis.

Decay chains evaluated were U-238→Th-234→Pa-234m→U-234→Th-230→Ra-226→Rn-222 and Pu-238→U-234→Th-230→Ra-226→Rn-222. Each parent in these chains, except Th-234 and Pa-234m, were simulated separately as the starting point of the decay chain. Th-234 and Pa-234m have extremely short half-lives compared to the other parent radionuclides in these chains. Only a fraction of the Rn-222 generated by the decay of each parent is available for migration away from its source and into open pore space. Since the Rn-222 parent radionuclides exist as oxides or in other crystalline forms, only a fraction of Rn-222 generated by decay of Ra-226 has sufficient energy to migrate away from its original location into adjacent pore space before further decay occurs (3.82 day half-life for Rn-222).

The emanation coefficient is generally defined as the fraction of the total amount of Rn-222 produced by radium decay that escapes from soil particles and enters the pore space of the medium. This is the fraction of the Rn-222 that is available for transport. In the case of the SDF, the parent radionuclides are not embedded in soil but are contained within waste mixed with grout. Literature values for the Rn-222 emanation factor for these conditions are not available. Studies have shown the emanation factor to vary between 0.02 and 0.7 for various soil types depending primarily on moisture content. Generally, higher emanation factors are associated with higher moisture contents.

RESRAD is a model used to estimate radiation dose and risk from residual radioactive materials. This USDOE and Nuclear Regulatory Commission (NRC) approved code, assumes an emanation factor of 0.25 for Rn-222 which is representative of a silty loam soil with a low moisture content. For the SDF radon pathway analysis, the RESRAD default emanation factor of 0.25 was chosen recognizing that literature values for wastes similar to the SDF are not available. To account for the emanation factor in the model, an effective source term of 0.25 Ci of parent radionuclide was utilized for each Ci disposed within the facility.

Some radon dissolves in pore water but since diffusion proceeds more slowly in that fluid, air diffusion was the only transport process by which Rn-222 was allowed to reach the land surface. This assertion is substantiated in Yu et al. (2001). In that report, the effective diffusion coefficient for soil is reported to range from the radon open air diffusion coefficient of 1.0×10^{-5} m^2/sec to that of fully saturated soil, 1.0×10^{-10} m^2/sec. This 5-order of magnitude difference is consistent with the comparison of water diffusion coefficients to air diffusion coefficients of other common molecular compounds and reported in many references. Thus, the larger volume of water-filled pore space compared to air-filled pore space (maximum of 1 order of magnitude

difference) is inconsequential, in terms of the ability of water-dissolved radon to diffuse through water-filled pores as compared to the ability of the same compounds to diffuse as gas in the vapor-filled pore spaces.

The molecular diffusion coefficient of Rn-222 in open air is 347 m^2/yr (Nielson et al., 1984). Nielson et al. (1984) established a relationship between moisture saturation and the radon effective air-diffusion coefficient for various pore sizes of earthen materials. This method was used to calculate a radon effective air-diffusion coefficient for each material type based upon the average moisture saturation for the material. Tortuosity was assigned a unit value for each material type. A summary of the radon air-diffusion coefficients by material type are presented in Table 12.

3.3.1 Radon Pathway Model Results

Model simulations were conducted to evaluate the peak instantaneous Rn-222 flux at the land surface for the simulation period of 10,000 years for each case simulated (i.e., one Ci of each parent). Model results were output in Ci/m^2/yr per Ci of inventory, consistent with the set of units employed in the model. Graphs of these results are shown in Figure 12 through Figure 16, although the units are converted to pCi/m^2/sec per Ci, which are the units used to define the regulatory flux limit in DOE M 435.1-1 (USDOE, 1999).

The material properties remained constant for each case for the simulation period. Hence, the transient gaseous flux of Rn-222 at the land surface is a function of radioactive decay. This is illustrated in Figure 12 through Figure 16 where the flux of Rn-222 reaches the peak emission rate and subsequently declines as a function of decay. The peak fluxes represent the peak Rn-222 flux per square meter at the land surface per Ci of parent. The peak fluxes are presented in Table 25 through Table 29.

4.0 SUMMARY

SRS is currently in the process of revising the Performance Assessment (PA) for the SDF as required by DOE Order 435.1, Radioactive Waste Management. As part of the PA process, an analysis was conducted to evaluate the potential magnitude of gaseous release of radionuclides from the SDF over the 10,000-year post-closure compliance period. Specifically, an air and radon pathways analysis has been conducted to estimate the flux of volatile radionuclides and radon at the ground surface due to waste stored in Vault 1, Vault 4, and future disposal units following closure. This analysis was used as the basis to estimate the dose to the maximally exposed individual (MEI) for the air pathway per Curie (Ci) of each radionuclide in each disposal unit.

For the air pathway analysis, several gaseous radionuclides were considered. These included carbon-14 (C-14), chlorine-36 (Cl-36), iodine-129 (I-129), selenium-79 (Se-79), antimony-125 (Sb-125), tin-126 (Sn-126), tritium (H-3), and technetium-99 (Tc-99). The dose to the MEI per Ci disposed was estimated at the SRS Boundary and at the 100 m compliance point.

For the radon pathway analysis, five parent radionuclides and their progeny were analyzed. These parent radionuclides included uranium-238 (U-238), plutonium-238 (Pu-238), uranium-234 (U-234), thorium-230 (Th-230), and radium-226 (Ra-226). The peak flux of radon-222 due to one Ci of each parent radionuclide was estimated for the simulation period of 10,000 years.

5.0 REFERENCES

ACRI (Analytical & Computational Research, Inc.). 2004. PORFLOW Version 5.0 User's Manual, Revision 5, Analytical & Computational Research, Inc., Los Angeles, California.

Bethke. C.M. 2005. The Geochemist's Workbench® (geochemical modeling software), Release 6.0, University of Illinois.

Bolz, R.E. and G.L. Tuve, (Editors), 1973. *Handbook of tables for APPLIED ENGINEERING SCIENCE, 2'nd Edition*. CRC Press, 18901 Cranwood Parkway, Cleveland, OH.

Denham, M. E. 2008. Estimation of Eh and pH Transitions in Pore Fluids During Aging of Saltstone and Vault 2 Concrete. SRNL-TR-2008-00283, Savannah River National Laboratory, Aiken, SC.

Dixon, K. L., J. R. Harbour, and M. A. Phifer. 2008. Hydraulic And Physical Properties Of Saltstone Grouts And Vault Concretes, SRNL-STI-2008-00421, Savannah River National Laboratory, Aiken, SC 29808.

Freeze, R. A. and J. A. Cherry. 1979. Groundwater. Prentice-Hall, Inc. Englewood Cliffs, NJ.

Glover, T. J. 2000. Pocket Ref, 2nd Edition. Sequoia Publishing, Inc. Littleton, CO.

Hillel, D. 1982. Introduction to Soil Physics, Academic Press, Inc., San Diego, California.

Jones, W. E. and M. A. Phifer. 2008. Saltstone Closure Facility Closure Cap and Concept and Infiltration Estimates, WSRC-STI-2008-00244. Washington Savannah River Company, Aiken, SC 29808.

Lee, P. L. and T. Q. Foley. 2008. Air Pathway Dose Modeling for the Saltstone Disposal Facility, SRNL-STI-2008-00415, Rev. 0. Savannah River National Laboratory, Aiken, SC 29808.

Nielson, K.K., V.C. Rogers and G.W. Gee, 1984. *Diffusion of Radon through Soils: A pore distribution Model*, Soil Science Society of America, J. 48:482-487.

Nordstrom, D.K. and J.L. Munoz. 1985. Geochemical Thermodynamics. The Benjamin/Cummings Publishing Co., Inc., Menlo Park, CA.

Phifer, M.A., M. A. Millings, G. P. Flach, 2006. Hydraulic Property Estimation for the E-Area and Z-Area Vadose Zone Soils, Cementitious Materials, and Waste Zones (U). WSRC-STI-2006-00198. Westinghouse Savannah River Company, Aiken, South Carolina. September 2003.

Tuli, J.K. 2005. Nuclear Wallet Cards, sixth edition, Brookhaven National Laboratory, Upton, New York.

USDOE, 1999. Radioactive Waste Management Manual, DOE M 435.1-1. U. S. Department of Energy, July 9, 1999.

WSRC. 2008. Saltstone Disposal Facility Radiological Screening Inputs, SDF-IP-09, Rev. 0, Washington Savannah River Company, Aiken, SC 29808.

Yu, C., A. J. Zielen, J. J. Cheng, D. J. LePoire, E. Gnanapragasam, S. Kamboj, J. Arnish, A. Wallo III, W. A. Williams, and H. Peterson, 2001. *Users Manual for RESRAD Version 6*, Environmental Assessment Division, Argonne National Laboratory. Chicago, Illinois.

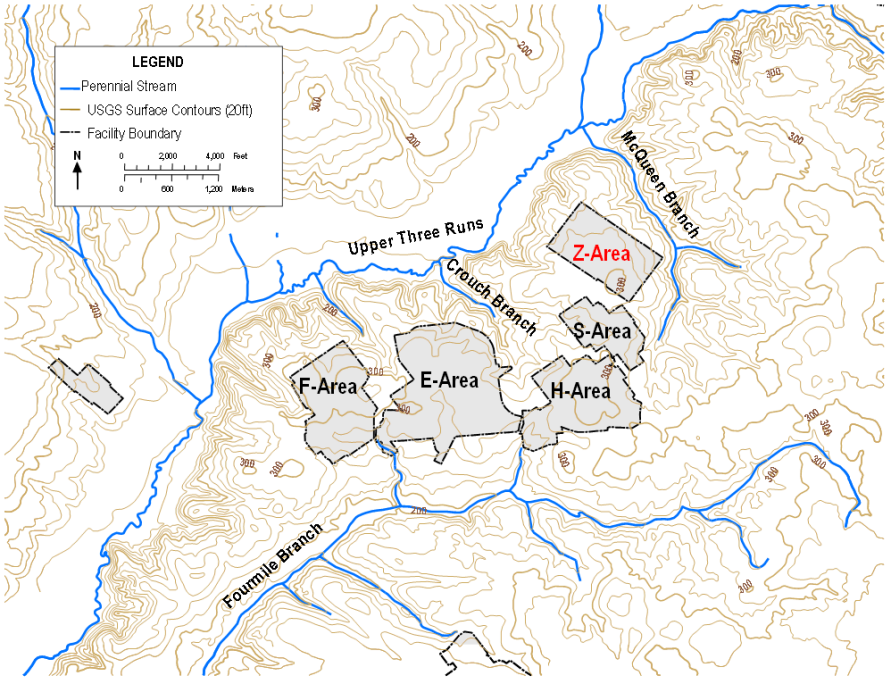

Figure 1. General Separations Area (GSA) Topography and Z-Area (SDF) Location

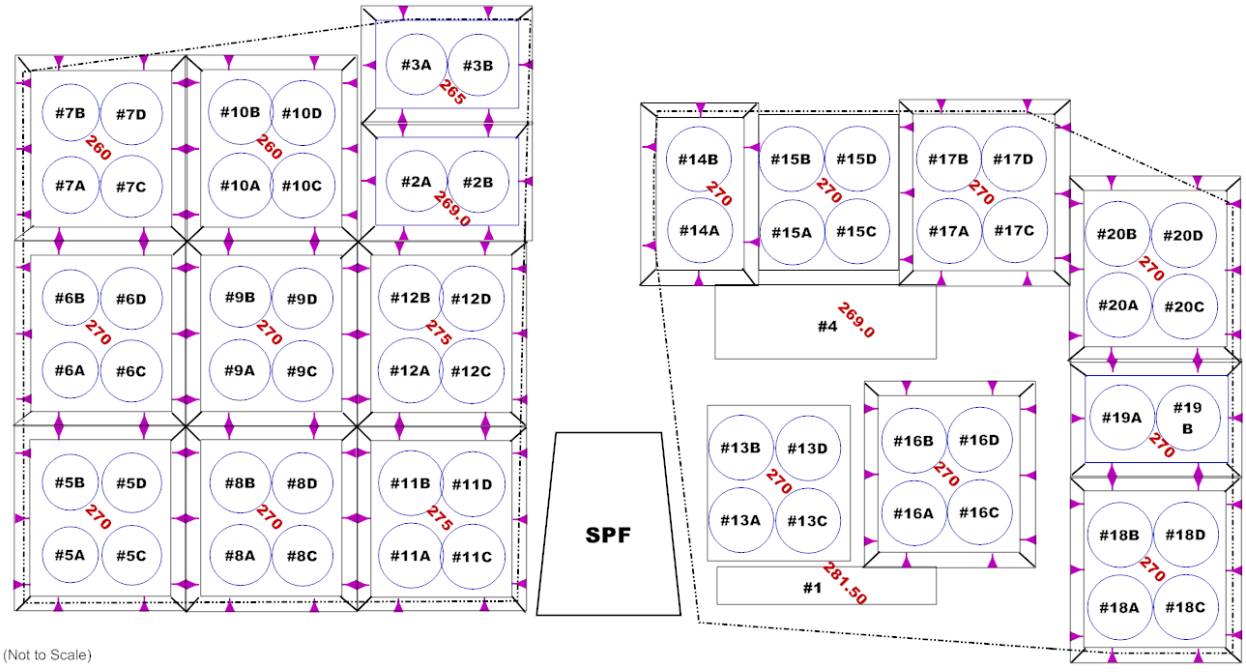

Figure 2. General Layout of the Saltstone Disposal Facility.

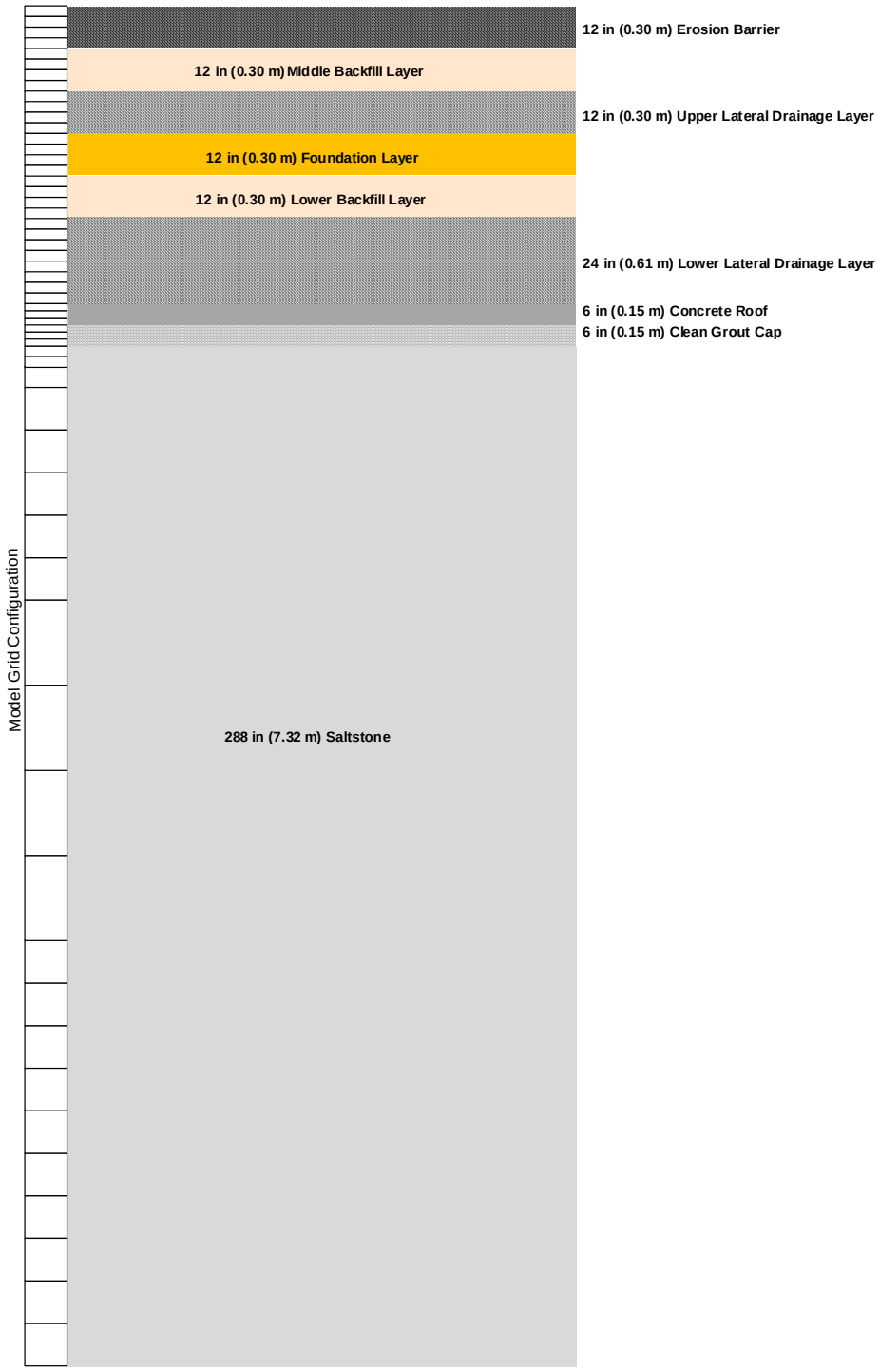

Figure 3. Schematic of PORFLOW Model Grid for the Vault 1 Air and Radon Pathway Analysis

Note: For conservatism the model grid does not include the following layers: topsoil, upper backfill, geotextile fabric, HPDE geomembrane, and GCL.

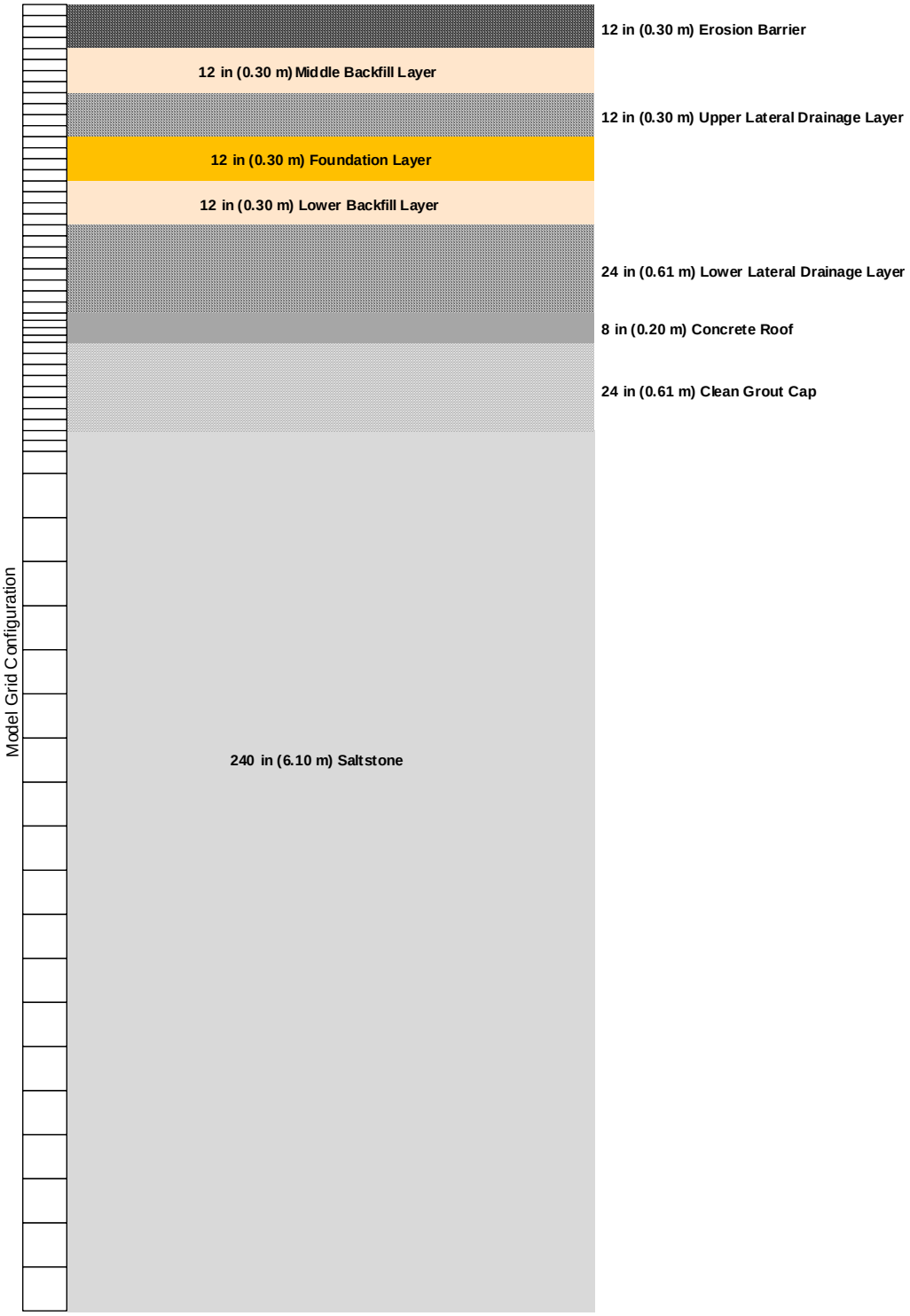

Figure 4. Schematic of PORFLOW Model Grid for the Vault 2 (and future disposal units) Air and Radon Pathway Analysis

Note: For conservatism the model grid does not include the following layers: topsoil, upper backfill, geotextile fabric, HPDE geomembrane, and GCL.

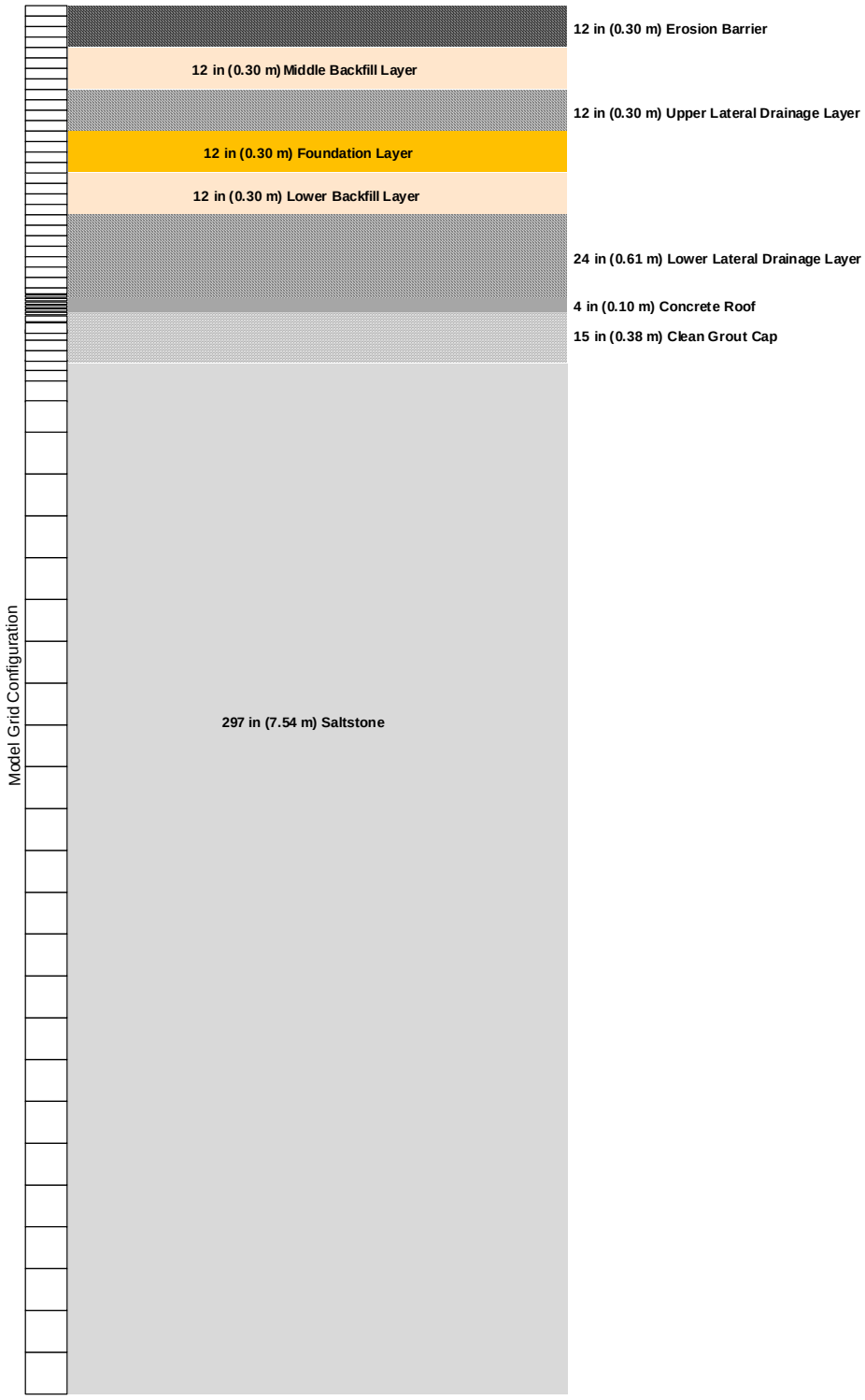

Figure 5. Schematic of PORFLOW Model Grid for the Vault 4 Air and Radon Pathway Analysis

Note: For conservatism the model grid does not include the following layers: topsoil, upper backfill, geotextile fabric, HPDE geomembrane, and GCL.

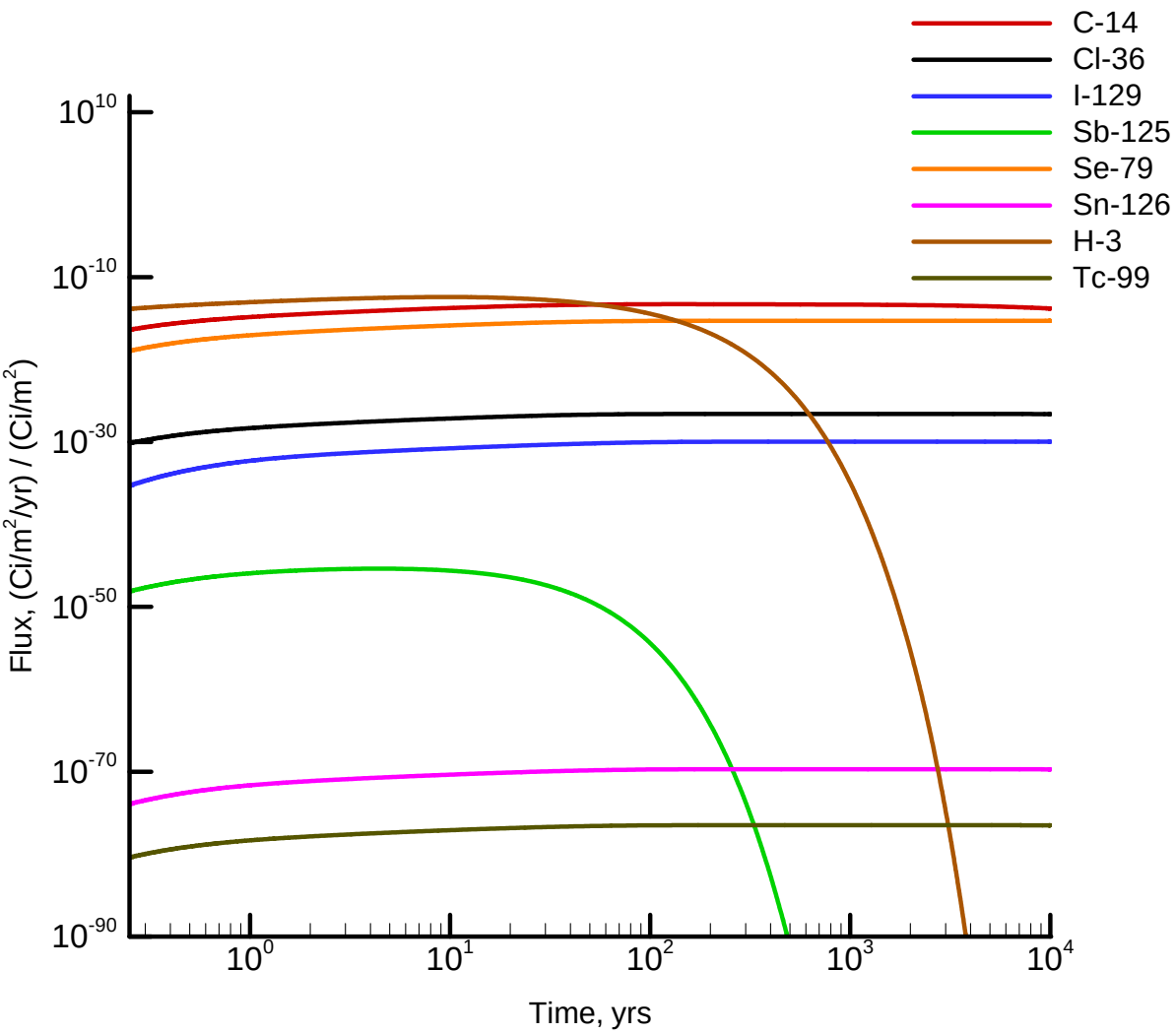

Figure 6. Flux at Land Surface for C-14, Cl-36, I-129, Sb-125, Se-79, Sn-126, H-3, and Tc-99 per Ci of Radionuclide in Vault 1 for DDA Saltstone.

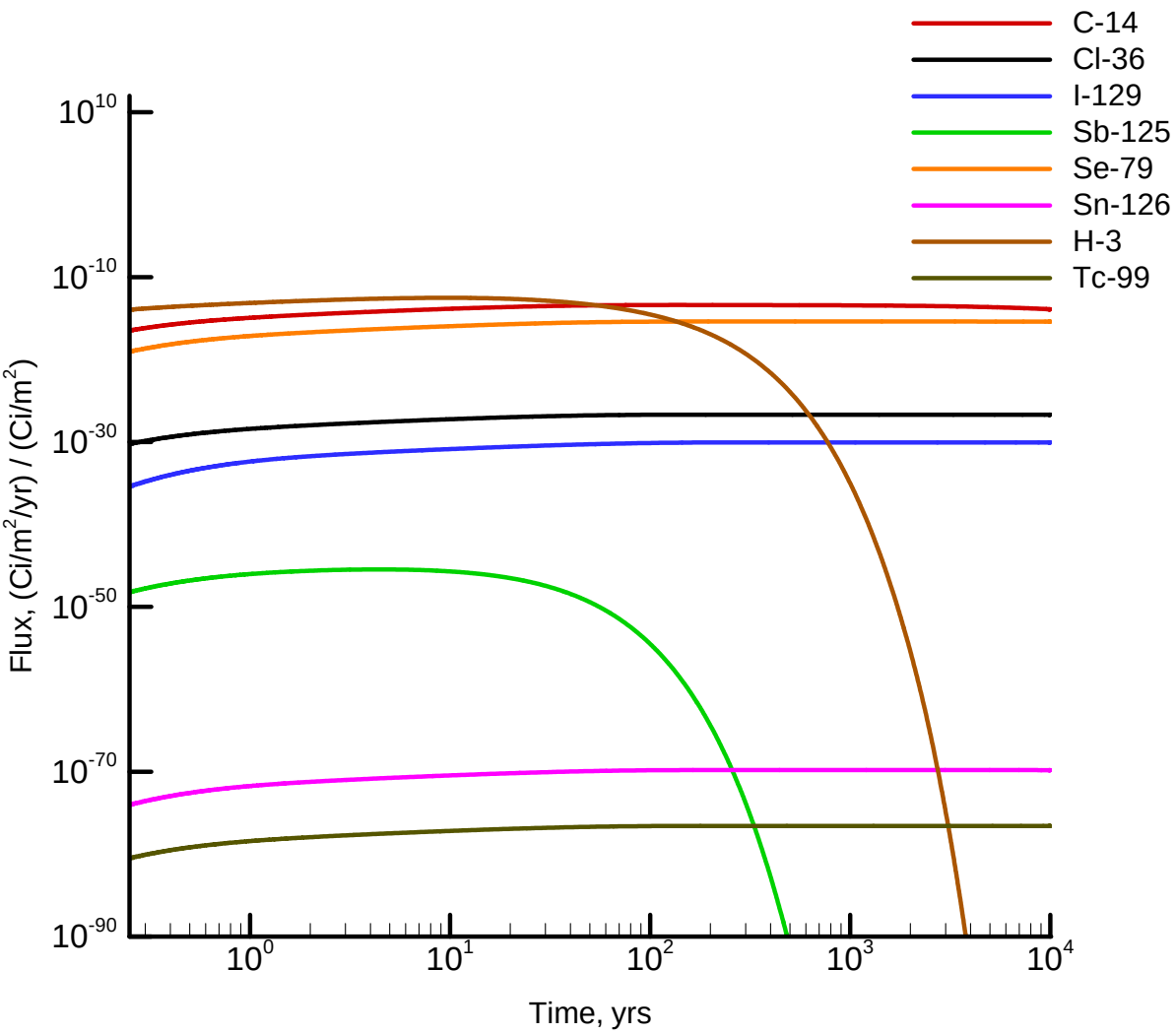

Figure 7. Flux at Land Surface for C-14, Cl-36, I-129, Sb-125, Se-79, Sn-126, H-3, and Tc-99 per Ci of Radionuclide in Vault 1 for ARP/MCU Saltstone.

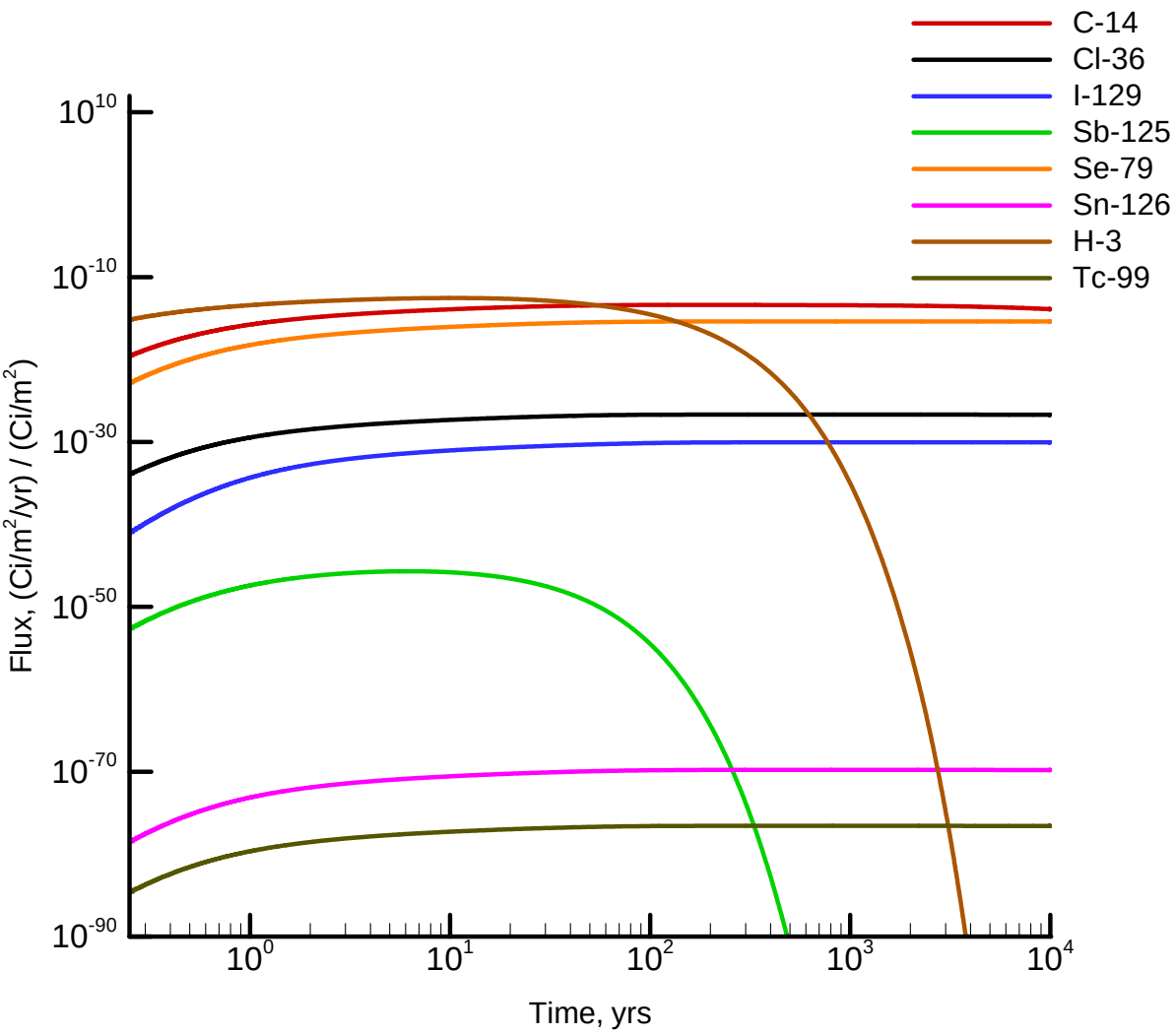

Figure 8. Flux at Land Surface for C-14, Cl-36, I-129, Sb-125, Se-79, Sn-126, H-3, and Tc-99 per Ci of Radionuclide in Vault 2 (and future disposal units) for SWPF Saltstone.

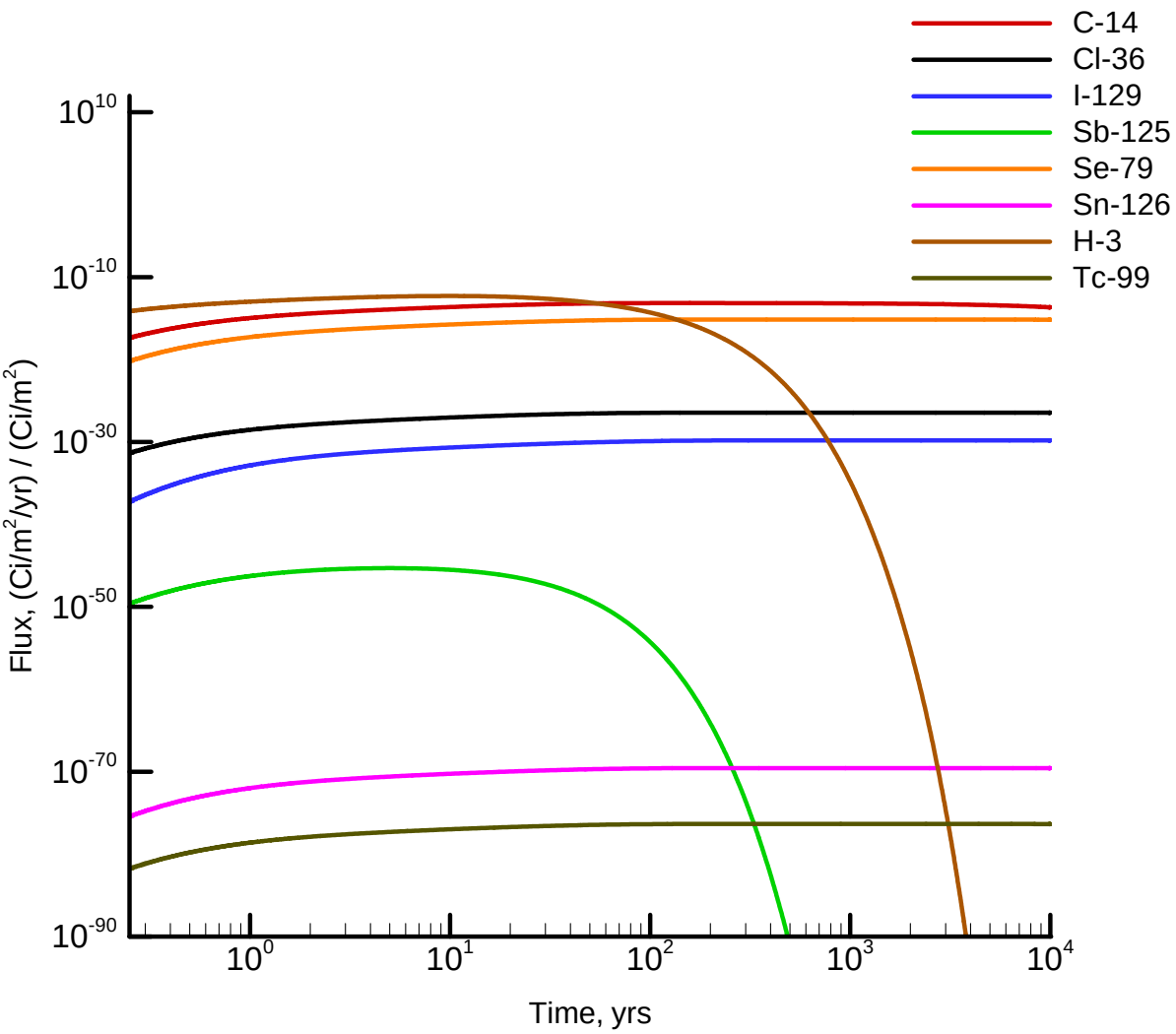

Figure 9. Flux at Land Surface for C-14, Cl-36, I-129, Sb-125, Se-79, Sn-126, H-3, and Tc-99 per Ci of Radionuclide in Vault 4 for DDA Saltstone.

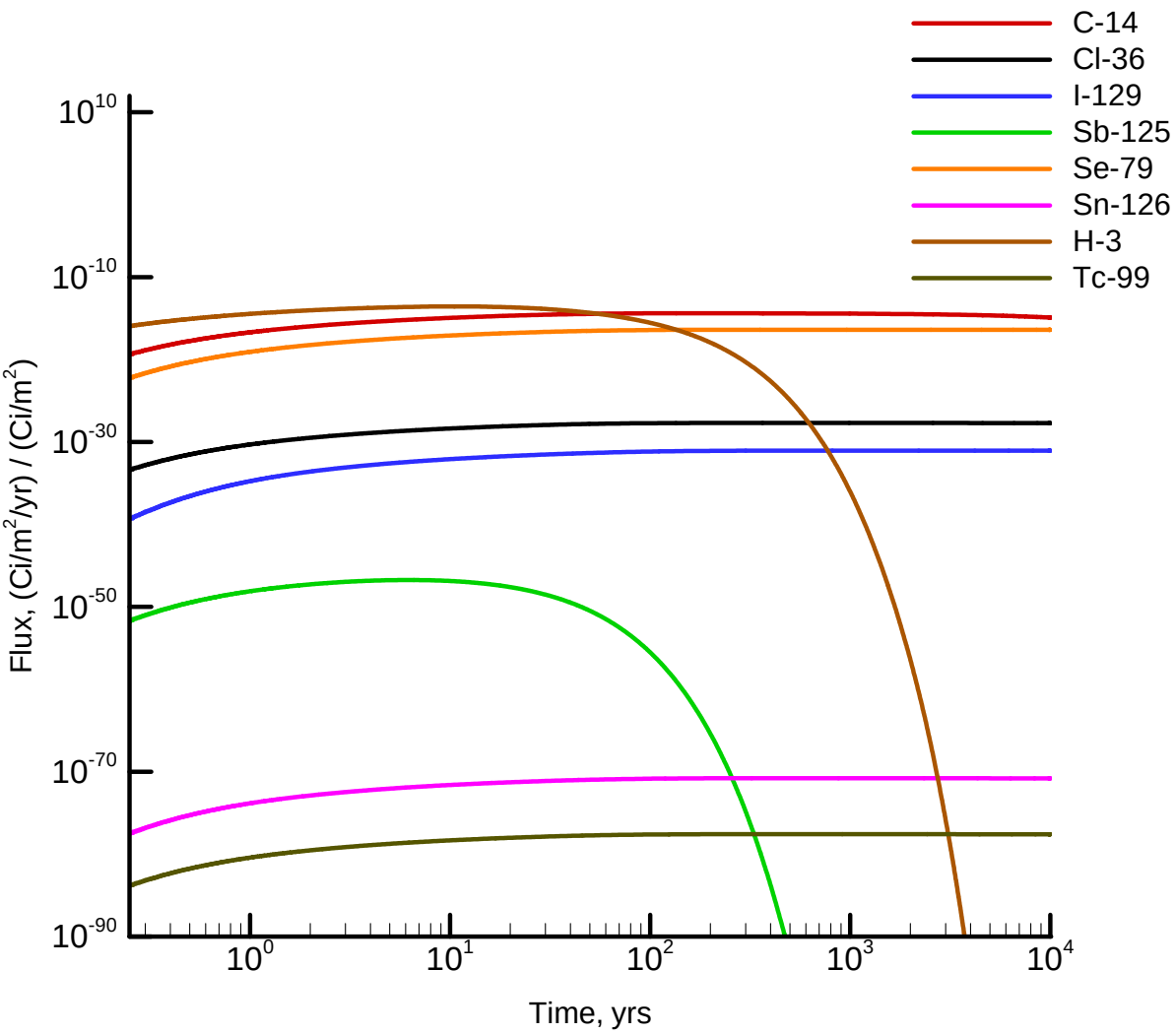

Figure 10. Flux at Land Surface for C-14, Cl-36, I-129, Sb-125, Se-79, Sn-126, H-3, and Tc-99 per Ci of Radionuclide in Vault 4 for ARP/MCU Saltstone.

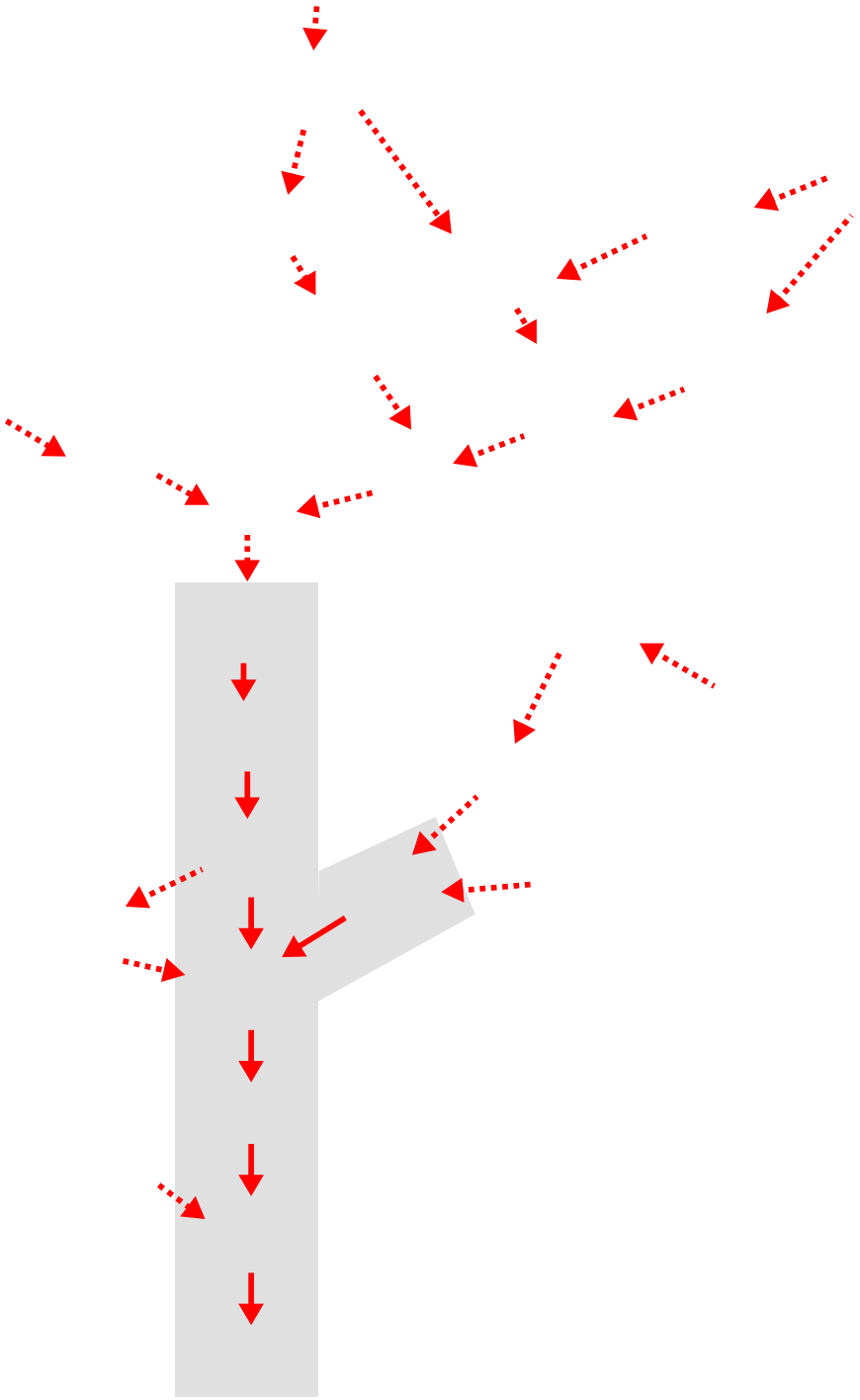

Figure 11. Radioactive Decay Chains Leading to Rn-222

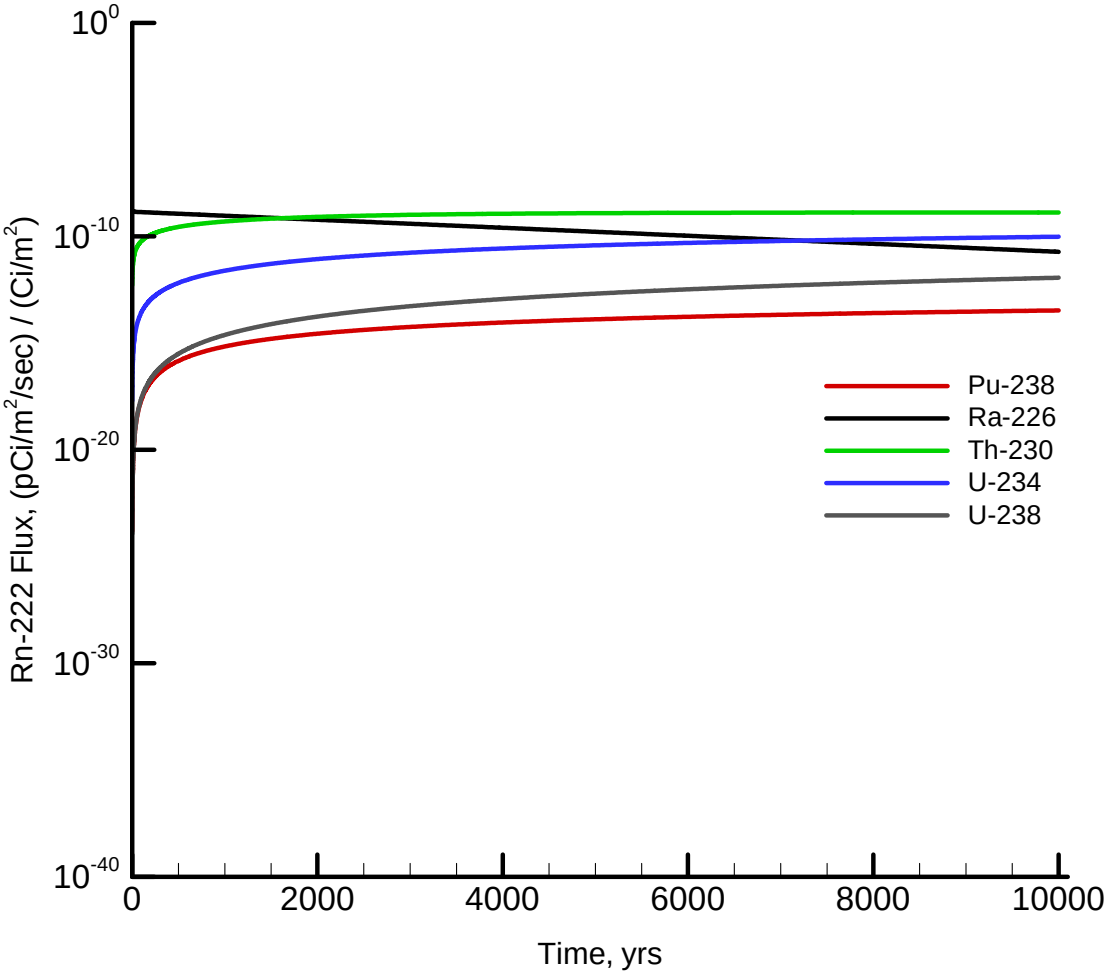

Figure 12. Rn-222 Flux at Land Surface Resulting from Unit Source Term for Vault 1 DDA Saltstone

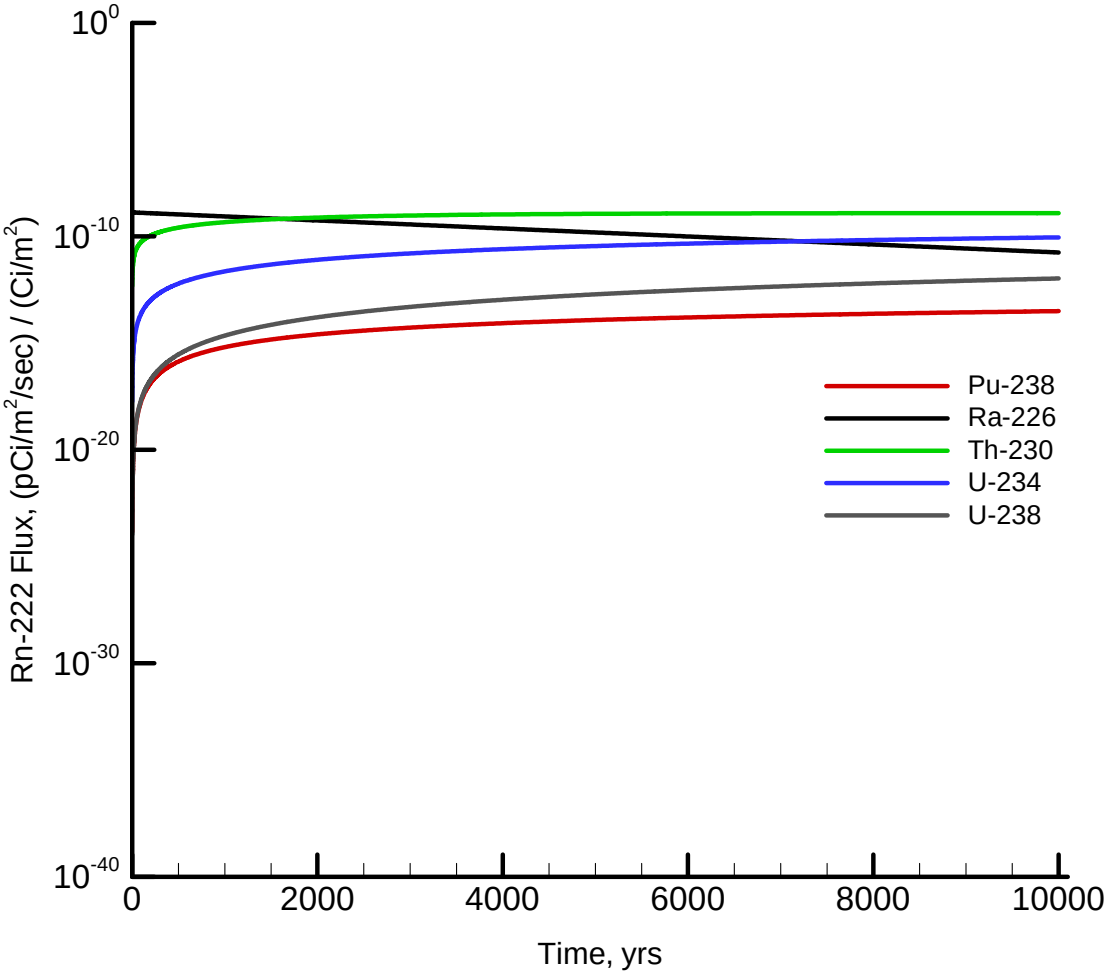

Figure 13. Rn-222 Flux at Land Surface Resulting from Unit Source Term for Vault 1 ARP/MCU Saltstone

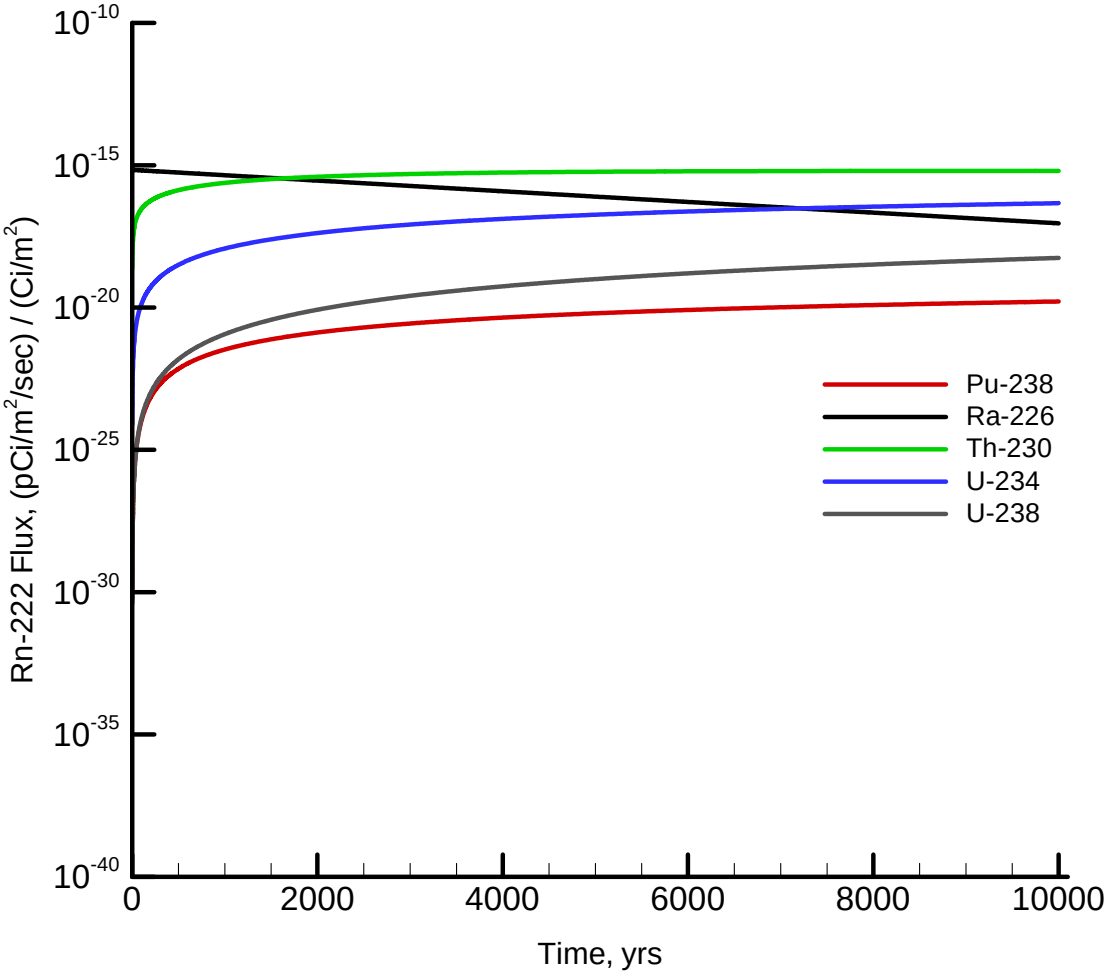

Figure 14. Rn-222 Flux at Land Surface Resulting from Unit Source Term for Vault 2 (and future disposal units) SWPF Saltstone

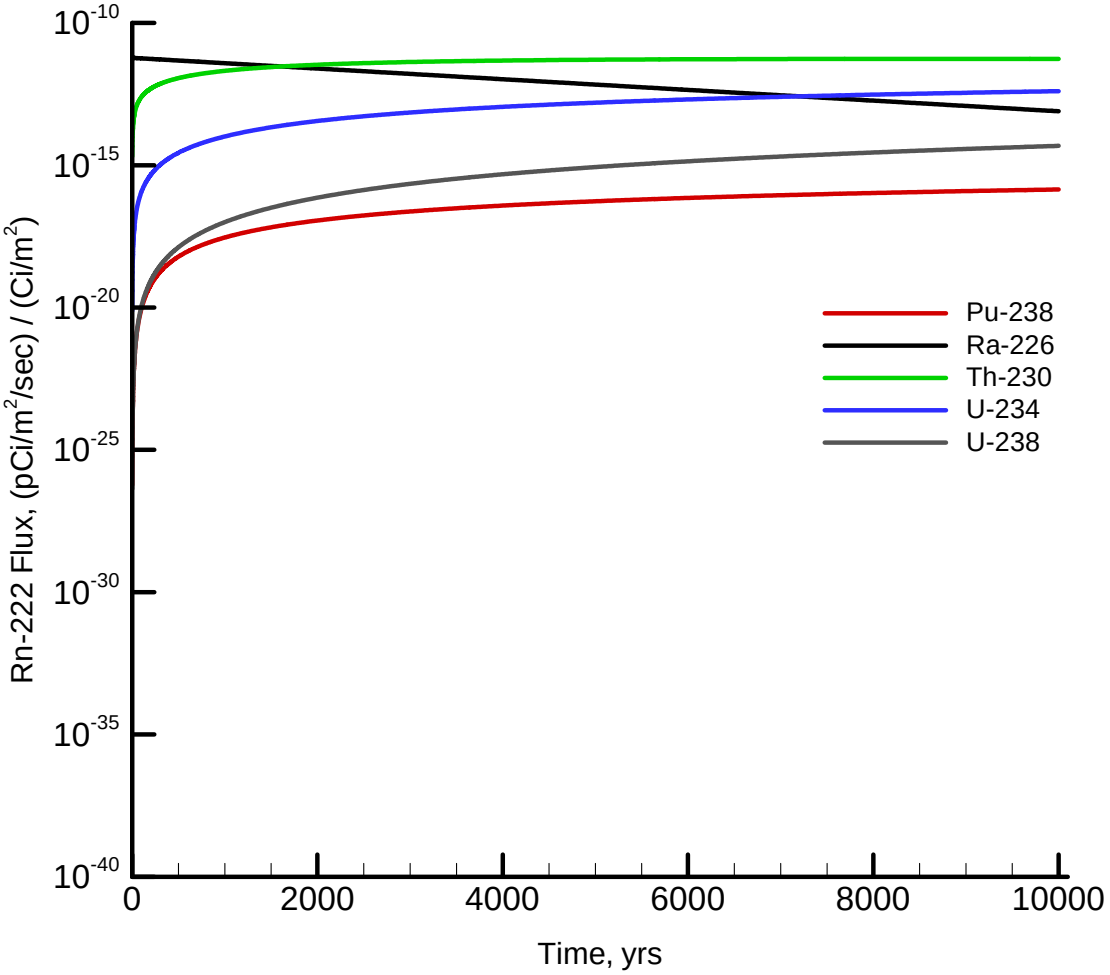

Figure 15. Rn-222 Flux at Land Surface Resulting from Unit Source Term for Vault 4 DDA Saltstone

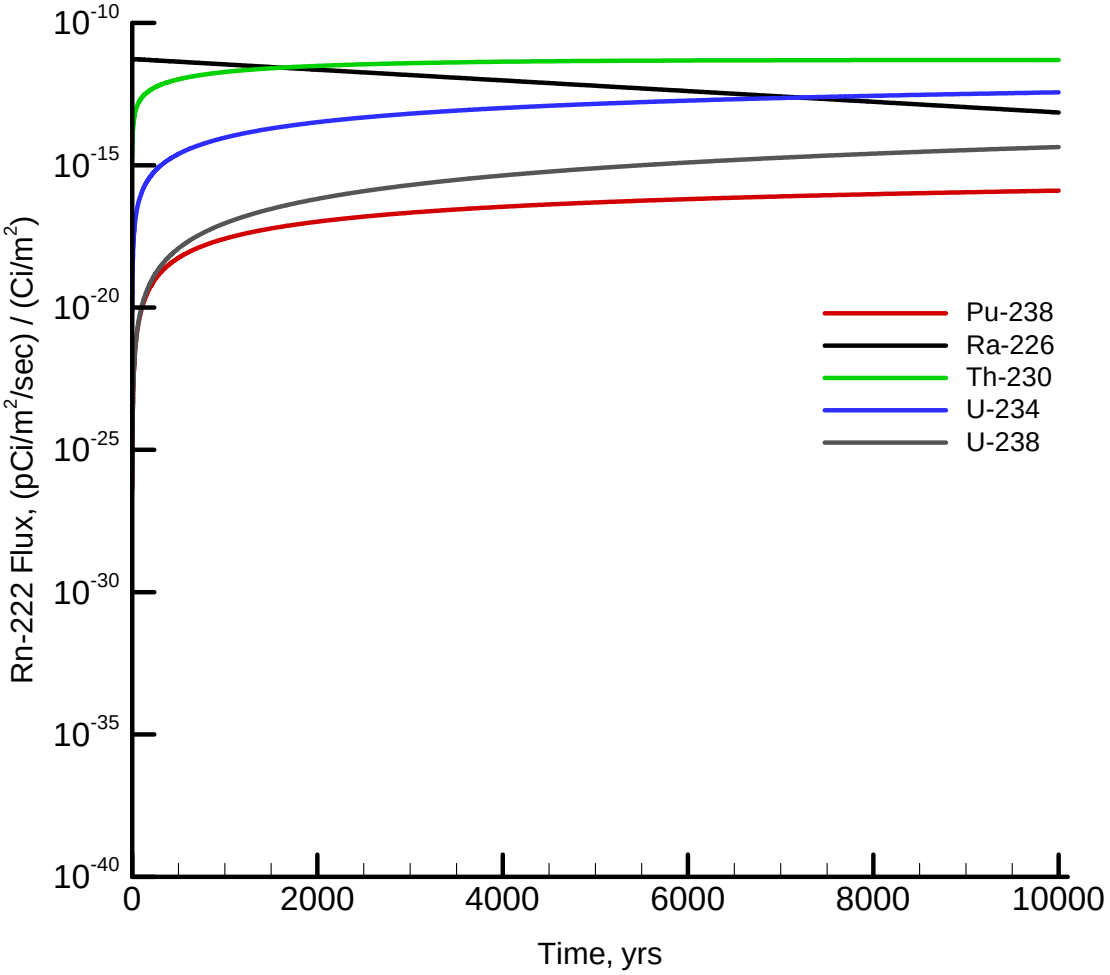

Figure 16. Rn-222 Flux at Land Surface Resulting from Unit Source Term for Vault 4 ARP/MCU Saltstone

Table 1. Vertical Layer Sequence and Associated Thickness for Vault 1 and Cover Material

Layer	Thickness (inches)	Thickness (ft)	Thickness (m)
Erosion barrier	12	1.00	0.30
Middle backfill layer	12	1.00	0.30
Upper lateral drainage layer	12	1.00	0.30
Foundation layer	12	1.00	0.30
Lower backfill layer	12	1.00	0.30
Lower drainage layer	24	2.00	0.61
Concrete Roof	6	0.50	0.15
Clean Grout	6	0.50	0.15
Saltstone (DDA or ARP/MCU)	288	24.00	7.32

SOURCE: Phifer et al. (2006).

Table 2. Vertical Layer Sequence and Associated Thickness for Vault 2 (and future disposal units) and Cover Material

Layer	Thickness (inches)	Thickness (ft)	Thickness (m)
Erosion barrier	12	1.00	0.30
Middle backfill layer	12	1.00	0.30
Upper lateral drainage layer	12	1.00	0.30
Foundation layer	12	1.00	0.30
Lower backfill layer	12	1.00	0.30
Lower drainage layer	24	2.00	0.61
Concrete Roof	8	0.67	0.20
Clean Grout	24	2.00	0.61
Saltstone (SWPF)	240	20.00	6.10

SOURCE: Phifer et al. (2006).

Table 3. Vertical Layer Sequence and Associated Thickness for Vault 4 and Cover Material

Layer	Thickness (inches)	Thickness (ft)	Thickness (m)
Erosion barrier	12	1.00	0.30
Middle backfill layer	12	1.00	0.30
Upper lateral drainage layer	12	1.00	0.30
Foundation layer	12	1.00	0.30
Lower backfill layer	12	1.00	0.30
Lower drainage layer	24	2.00	0.61
Concrete Roof	4	0.33	0.10
Clean Grout	15	1.25	0.38
Saltstone (DDA or ARP/MCU)	297	24.75	7.55

SOURCE: Phifer et al. (2006).

Table 4. Particle Density, Total Porosity, Average Saturation, and Air-Filled Porosity by Layer for Vault 1.

Layer	Particle Density (g/cm^3)	Total Porosity (fraction)	Average Saturation (fraction)	Air-filled Porosity (fraction)
Erosion barrier[1, 3]	2.65	0.150	0.88	0.017
Middle backfill layer[2, 3]	2.63	0.350	0.96	0.012
Upper lateral drainage layer[1, 3]	2.65	0.417	0.61	0.162
Foundation layer[2, 3]	2.63	0.350	0.86	0.048
Lower backfill layer[2, 3]	2.63	0.350	0.76	0.082
Lower drainage layer[1, 3]	2.65	0.417	0.00	0.417
Concrete Roof[4,7]	2.53	0.120	0.98	0.032
Clean Grout DDA[5, 7]	2.37	0.550	0.98	0.011
Clean Grout ARP/MCU[5, 7]	2.38	0.590	0.98	0.012
DDA Saltstone[6, 7]	2.37	0.550	0.98	0.011
ARP/MCU Saltstone[6, 7]	2.38	0.590	0.98	0.012

[1]Particle density assumed to be that typical of quartz (Hillel, 1982)
[2]Values for particle density taken as that of control compacted backfill from Phifer et al. (2006).
[3]Total porosity, average saturation, and air-filled porosity values derived from Jones and Phifer (2008).
[4]Values for total porosity and particle density for the Vault 1 concrete roof taken from Dixon et al. (2008).
[5]Particle density and porosity of clean grout assumed to be the same as saltstone and taken from Dixon et al. (2008).
[6]The particle density and total porosity of the DDA and ARP/MCU saltstone were taken from Dixon et al. (2008).
[7]The concrete roof, clean grout, and saltstone waste layers were assigned average saturation values based on the SDF PA vadose zone flow model.

Table 5. Particle Density, Total Porosity, Average Saturation, and Air-Filled Porosity by Layer for Vault 2 (and future disposal units)

Layer	Particle Density (g/cm^3)	Total Porosity (fraction)	Average Saturation (fraction)	Air-filled Porosity (fraction)
Erosion barrier[1, 3]	2.65	0.150	0.88	0.017
Middle backfill layer[2, 3]	2.63	0.350	0.96	0.012
Upper lateral drainage layer[1, 3]	2.65	0.417	0.61	0.162
Foundation layer[2, 3]	2.63	0.350	0.86	0.048
Lower backfill layer[2, 3]	2.63	0.350	0.76	0.082
Lower drainage layer[1, 3]	2.65	0.417	0.00	0.417
Concrete Roof[4,7]	2.50	0.110	0.98	0.002
Clean Grout[5, 7]	2.42	0.580	0.99	0.009
SWPF Saltstone[6, 7]	2.42	0.580	0.99	0.009

[1]Particle density assumed to be that typical of quartz (Hillel, 1982)
[2]Values for particle density taken as that of control compacted backfill from Phifer et al. (2006).
[3]Total porosity, average saturation, and air-filled porosity values derived from Jones and Phifer (2008).
[4]Values for total porosity and particle density for the Vault 1 concrete roof taken from Dixon et al. (2008).
[5]Particle density and porosity of clean grout assumed to be the same as saltstone and taken from Dixon et al. (2008).
[6]The particle density and total porosity of the SWPF saltstone were taken from Dixon et al. (2008).
[7]The concrete roof, clean grout, and saltstone waste layers were assigned average saturation values based on the SDF PA vadose zone flow model.

Table 6. Particle Density, Total Porosity, Average Saturation, and Air-Filled Porosity by Layer for Vault 4

Layer	Particle Density (g/cm^3)	Total Porosity (fraction)	Average Saturation (fraction)	Air-filled Porosity (fraction)
Erosion barrier[1, 3]	2.65	0.150	0.88	0.017
Middle backfill layer[2, 3]	2.63	0.350	0.96	0.012
Upper lateral drainage layer[1, 3]	2.65	0.417	0.61	0.162
Foundation layer[2, 3]	2.63	0.350	0.86	0.048
Lower backfill layer[2, 3]	2.63	0.350	0.76	0.082
Lower drainage layer[1, 3]	2.65	0.417	0.00	0.417
Concrete Roof[4,7]	2.53	0.120	0.98	0.002
Clean Grout DDA[5, 7]	2.37	0.550	0.99	0.008
Clean Grout ARP/MCU[5, 7]	2.38	0.590	0.99	0.009
DDA Saltstone[6, 7]	2.37	0.550	0.99	0.008
ARP/MCU Saltstone[6, 7]	2.38	0.590	0.99	0.009

[1]Particle density assumed to be that typical of quartz (Hillel, 1982)
[2]Values for particle density taken as that of control compacted backfill from Phifer et al. (2006).
[3]Total porosity, average saturation, and air-filled porosity values derived from Jones and Phifer (2008).
[4]Values for total porosity and particle density for the Vault 1 concrete roof taken from Dixon et al. (2008).
[5]Particle density and porosity of clean grout assumed to be the same as saltstone and taken from Dixon et al. (2008).
[6]The particle density and total porosity of the DDA and ARP/MCU saltstone were taken from Dixon et al. (2008).
[7]The concrete roof, clean grout, and saltstone waste layers were assigned average saturation values based on the SDF PA vadose zone flow model.

Table 7. Radionuclides and Compounds of Interest for Air and Radon Pathway Analysis

Radionuclide	Half-life[1] (yrs)	Approximate Atomic Wt.[2]	Molecular form in gaseous state	Molecular Wt.[2]
$^{14}CO_2$	5.700E+03	14	CO_2	45.99
2(^{36}Cl)	3.010E+05	36	Cl_2	72
2(^{129}I)	1.570E+07	129	I_2	258
^{125}Sb	2.759E+00	125	Sb	125
^{79}Se	2.950E+05	79	Se	79
^{126}Sn	2.300E+05	126	Sn	126
$^{3}H_2$	12.32E+00	3	H_2	6
^{99}Tc	2.111E+05	99	Tc	99
^{222}Rn	1.047E-02	222	Rn	222

[1]2005 Nuclear Wallet Cards (Tuli, 2005)
[2]Pocket Ref (Glover, 2000)

Table 8. Gases Considered for Each Radionuclide, their Reaction with their Aqueous Component, and the Equilibrium Constants for Each Reaction used in The Geochemist's Workbench®

Contaminant	Gas Species	Reaction	Log K (25°C)
C-14	CO_2	$CO_{2(g)} + H_2O = HCO_3^- + H^+$	-7.82
Cl-36	Cl_2	$Cl_{2(g)} + H_2O = 2Cl^- + 2H^+ + ½O_2$	3.03
Cl-36	$HClO_4$	$HClO_{4(g)} = Cl^- + 2O_2 + H^+$	33.38
Cl-36	HCl	$HCl_{(g)} = Cl^- + H^+$	6.31
H-3	H_2O	$H_2O_{(g)} = H_2O_{(l)}$	1.50
I-129	I_2	$I_{2(g)} + H_2O = 2I^- + ½O_2 + 2H^+$	-21.53
I-129	HI	$HI_{(g)} = I^- + H^+$	9.31
Sb-125, 126	$SbCl_3$	$SbCl_{3(g)} + 3H_2O = Sb(OH)_3^o + 3Cl^- + 3H^+$	4.83
Sb-125, 126	$SbCl_5$	$SbCl_{5(g)} + 4H_2O = Sb(OH)_3^o + 5Cl^- + ½O_2 + 5H^+$	2.74
Sb-125, 126	SbH_3	$SbH_{3(g)} + 3/2O_2 = Sb(OH)_3^o$	143.11
Se-79	H_2Se	$H_2Se_{(g)} + 3/2O_2 = SeO_3^{-2} + 2H^+$	71.83
Se-79	$SeCl_4$	$SeCl_{4(g)} + 3H_2O = SeO_3^{-2} + 4Cl^- + 6H^+$	13.78
Sn-121m, 126	$SnCl_4$	$SnCl_{4(g)} = Sn^{+4} + 4Cl^-$	15.85
Sn-121m, 126	SnH_4	$SnH_{4(g)} + 4H^+ = 4H_2 + Sn^{+4}$	20.10

Table 9. Parameters Used in Estimating Apparent Henry's Law Constants

Parameter	Value Used
pH	11.0
Eh	-0.45 V
Na+	0.01 moles/kg
Cl-	0.01 moles/kg
T	25°C

Table 10. Radionuclides of Interest, the Dominant Gas Under Saltstone Conditions, and the Apparent Henry's Law Constant for Each Radionuclide

Radionuclide	Gas	H (mole/atm-kg)
Tritium	Water Vapor	2.1×10^{3}
C-14	CO_2	1.4×10^{4}
Cl-36	HCl	2.3×10^{17}
I-129	HI	2.8×10^{20}
Tc-99	Tc_2O_7	1.5×10^{67}
Sn-121m, 126	SnH_4	2.2×10^{60}
Sb-125, 126	SbH_3	3.3×10^{34}
Se-79	H_2Se	1.1×10^{6}

Table 11. Apparent Henry's Law Constant and Partitioning Coefficient (K_d) for Each Radionuclide

Radionuclide	H (mole/atm-kg)	K_d (ml/g)
Tritium	2.1×10^{3}	5.05×10^{4}
C-14	1.4×10^{4}	3.37×10^{5}
Cl-36	2.3×10^{17}	5.53×10^{18}
I-129	2.8×10^{20}	6.73×10^{21}
Tc-99	1.5×10^{67}	3.61×10^{68}
Sn-121m, 126	2.2×10^{60}	5.29×10^{61}
Sb-125, 126	3.3×10^{34}	7.93×10^{35}
Se-79	1.1×10^{6}	3.61×10^{7}

Table 12. Effective Air-Diffusion Coefficients for Each Radionuclide/Compound, by Material for Vault 1 and Closure Cap

Radionuclide[1,2]	Saltstone and Clean Grout Layer (m^2/yr)	Concrete Roof (m^2/yr)	Lower Drainage Layer (m^2/yr)	Lower Backfill Layer (m^2/yr)	Foundation Layer (m^2/yr)	Upper Lateral Drainage Layer (m^2/yr)	Middle Backfill Layer (m^2/yr)	Erosion Barrier Layer (m^2/yr)
^{222}Rn	8.79E-02	8.79E-02	3.47E+02	2.05E+00	1.09E+00	4.20E+00	1.77E-01	9.17E-01
^{14}C	1.93E-01	1.93E-01	7.62E+02	4.51E+00	2.40E+00	2.40E+00	9.23E+00	3.88E-01
^{36}Cl	1.54E-01	1.54E-01	6.09E+02	3.61E+00	1.92E+00	7.38E+00	3.10E-01	1.61E+00
^{129}I	8.16E-02	8.16E-02	3.22E+02	1.91E+00	1.01E+00	3.90E+00	1.64E-01	8.50E-01
^{125}Sb	1.17E-01	1.17E-01	4.62E+02	2.74E+00	1.45E+00	5.60E+00	2.36E-01	1.22E+00
^{126}Sb	1.17E-01	1.17E-01	4.61E+02	2.73E+00	1.45E+00	5.58E+00	2.35E-01	1.22E+00
^{79}Se	1.47E-01	1.47E-01	5.82E+02	3.44E+00	1.83E+00	7.05E+00	2.96E-01	1.54E+00
^{126}Sn	1.17E-01	1.17E-01	4.61E+02	2.73E+00	1.45E+00	5.58E+00	2.35E-01	1.22E+00
$^{3}H_2$	5.35E-01	5.35E-01	2.11E+03	1.25E+01	6.64E+00	2.56E+01	1.07E+00	5.58E+00
^{99}Tc	1.32E-01	1.32E-01	5.20E+02	3.08E+00	1.63E+00	6.29E+00	2.65E-01	1.37E+00

[1]The effective diffusion coefficient for ^{222}Rn was used to determine the effective air diffusion coefficient of each radionuclide/compound based on Graham's law.
[2]The effective diffusion coefficients for all three disposal units are the same because the average saturation assumed for each layer is the same for all three designs.

Table 13. Effective Air-Diffusion Coefficients for Each Radionuclide/Compound, by Material for Vault 2 (and future disposal units) and Closure Cap

Radionuclide[1,2]	Saltstone and Clean Grout Layer (m^2/yr)	Concrete Roof (m^2/yr)	Lower Drainage Layer (m^2/yr)	Lower Backfill Layer (m^2/yr)	Foundation Layer (m^2/yr)	Upper Lateral Drainage Layer (m^2/yr)	Middle Backfill Layer (m^2/yr)	Erosion Barrier Layer (m^2/yr)
^{222}Rn	6.50E-02	6.50E-02	3.47E+02	2.05E+00	1.09E+00	4.20E+00	1.77E-01	9.17E-01
^{14}C	1.43E-01	1.43E-01	7.62E+02	4.51E+00	2.40E+00	2.40E+00	9.23E+00	3.88E-01
^{36}Cl	1.14E-01	1.14E-01	6.09E+02	3.61E+00	1.92E+00	7.38E+00	3.10E-01	1.61E+00
^{129}I	6.03E-02	6.03E-02	3.22E+02	1.91E+00	1.01E+00	3.90E+00	1.64E-01	8.50E-01
^{125}Sb	8.67E-02	8.67E-02	4.62E+02	2.74E+00	1.45E+00	5.60E+00	2.36E-01	1.22E+00
^{126}Sb	8.63E-02	8.63E-02	4.61E+02	2.73E+00	1.45E+00	5.58E+00	2.35E-01	1.22E+00
^{79}Se	1.09E-01	1.09E-01	5.82E+02	3.44E+00	1.83E+00	7.05E+00	2.96E-01	1.54E+00
^{126}Sn	8.63E-02	8.63E-02	4.61E+02	2.73E+00	1.45E+00	5.58E+00	2.35E-01	1.22E+00
$^{3}H_2$	3.96E-01	3.96E-01	2.11E+03	1.25E+01	6.64E+00	2.56E+01	1.07E+00	5.58E+00
^{99}Tc	9.74E-02	9.74E-02	5.20E+02	3.08E+00	1.63E+00	6.29E+00	2.65E-01	1.37E+00

[1]The effective diffusion coefficient for ^{222}Rn was used to determine the effective air diffusion coefficient of each radionuclide/compound based on Graham's law.
[2]The effective diffusion coefficients for all three disposal units are the same because the average saturation assumed for each layer is the same for all three designs.

Table 14. Effective Air-Diffusion Coefficients for Each Radionuclide/Compound, by Material for Vault 4 and Closure Cap

Radionuclide[1,2]	Saltstone and Clean Grout Layer (m^2/yr)	Concrete Roof (m^2/yr)	Lower Drainage Layer (m^2/yr)	Lower Backfill Layer (m^2/yr)	Foundation Layer (m^2/yr)	Upper Lateral Drainage Layer (m^2/yr)	Middle Backfill Layer (m^2/yr)	Erosion Barrier Layer (m^2/yr)
^{222}Rn	6.50E-02	6.50E-02	3.47E+02	2.05E+00	1.09E+00	4.20E+00	1.77E-01	9.17E-01
^{14}C	1.43E-01	1.43E-01	7.62E+02	4.51E+00	2.40E+00	9.23E+00	3.88E-01	2.01E+00
^{36}Cl	1.14E-01	1.14E-01	6.09E+02	3.61E+00	1.92E+00	7.38E+00	3.10E-01	1.61E+00
^{129}I	6.03E-02	6.03E-02	3.22E+02	1.91E+00	1.01E+00	3.90E+00	1.64E-01	8.50E-01
^{125}Sb	8.67E-02	8.67E-02	4.62E+02	2.74E+00	1.45E+00	5.60E+00	2.36E-01	1.22E+00
^{126}Sb	8.63E-02	8.63E-02	4.61E+02	2.73E+00	1.45E+00	5.58E+00	2.35E-01	1.22E+00
^{79}Se	1.09E-01	1.09E-01	5.82E+02	3.44E+00	1.83E+00	7.05E+00	2.96E-01	1.54E+00
^{126}Sn	8.63E-02	8.63E-02	4.61E+02	2.73E+00	1.45E+00	5.58E+00	2.35E-01	1.22E+00
$^{3}H_2$	3.96E-01	3.96E-01	2.11E+03	1.25E+01	6.64E+00	2.56E+01	1.07E+00	5.58E+00
^{99}Tc	9.74E-02	9.74E-02	5.20E+02	3.08E+00	1.63E+00	6.29E+00	2.65E-01	1.37E+00

[1]The effective diffusion coefficient for ^{222}Rn was used to determine the effective air diffusion coefficient of each radionuclide/compound based on Graham's law.
[2]The effective diffusion coefficients for all three disposal units are the same because the average saturation assumed for each layer is the same for all three designs.

Table 15. Peak Fluxes, Time to Peak Fluxes, SRS Boundary Dose Release Factors, and SRS Boundary Dose to the MEI for DDA Saltstone in Vault 1

Radionuclide	Peak Flux ($Ci/m^2/yr$) /Ci/m^2)	Time to Peak Flux (yrs)	SRS Boundary Dose Release Factor[1] (mrem/Ci)	Dose to MEI at SRS Boundary[2] (mrem/yr/Ci)
^{14}C	5.17E-14	136.7	1.1E-04	5.6E-18
^{36}Cl	2.56E-27	281.7	3.6E-04	9.3E-31
^{129}I	1.12E-30	763.8	4.8E-02	5.3E-32
^{125}Sb	4.33E-46	4.4	6.6E-03	2.9E-48
^{79}Se	5.12E-16	291.7	6.0E-04	3.1E-19
^{126}Sn	2.03E-70	350.8	3.0E-01	6.2E-71
$^{3}H_2$	3.85E-13	9.7	2.3E-06	8.7E-19
^{99}Tc	3.36E-77	311.2	1.8E-03	6.0E-80

[1]From Lee and Foley (2008).
[2] Dose to MEI at SRS Boundary = Peak Flux × SRS Boundary Dose Release Factor.
[3]Disposal Limit = 10 mrem/yr / Dose to MEI at SRS Boundary per Year per Ci

Table 16. Peak Fluxes, Time to Peak Fluxes, 100 m Dose Release Factors, and 100 m Boundary Dose to the MEI for DDA Saltstone in Vault 1

Radionuclide	Peak Flux ($Ci/m^2/yr$) /Ci/m^2)	Time to Peak Flux (yrs)	100 m Boundary Dose Release Factor[1] (mrem/Ci)	Dose to MEI at 100 m Boundary[2] (mrem/yr/Ci)
^{14}C	5.17E-14	136.7	3.7E-03	1.9E-16
^{36}Cl	2.56E-27	281.7	7.9E-03	2.0E-29
^{129}I	1.12E-30	763.8	5.5E+00	6.1E-30
^{125}Sb	4.33E-46	4.4	1.1E-01	4.8E-47
^{79}Se	5.12E-16	291.7	1.1E-02	5.6E-18
^{126}Sn	2.03E-70	350.8	4.9E+00	1.0E-69
$^{3}H_2$	3.85E-13	9.7	7.7E-05	3.0E-17
^{99}Tc	3.36E-77	311.2	2.9E-02	9.7E-79

[1]From Lee and Foley (2008).
[2] Dose to MEI at 100 m Boundary = Peak Flux × 100 m Boundary Dose Release Factor.
[3]Disposal Limit = 10 mrem/yr / Dose to MEI at 100 m Boundary per Year per Ci

Table 17. Peak Fluxes, Time to Peak Fluxes, SRS Boundary Dose Release Factors, and SRS Boundary Dose to the MEI for ARP/MCU Saltstone in Vault 1

Radionuclide	Peak Flux ($Ci/m^2/yr$) /Ci/m^2)	Time to Peak Flux (yrs)	SRS Boundary Dose Release Factor[1] (mrem/Ci)	Dose to MEI at SRS Boundary[2] (mrem/yr/Ci)
^{14}C	4.18E-14	136.0	1.1E-04	4.6E-18
^{36}Cl	2.07E-27	283.1	3.6E-04	7.5E-31
^{129}I	9.02E-31	715.8	4.8E-02	4.3E-32
^{125}Sb	3.51E-46	4.4	6.6E-03	2.3E-48
^{79}Se	4.14E-16	291.7	6.0E-04	2.5E-19
^{126}Sn	1.64E-70	350.8	3.0E-01	5.0E-71
$^{3}H_2$	3.12E-13	9.7	2.3E-06	7.1E-19
^{99}Tc	2.72E-77	311.2	1.8E-03	4.9E-80

[1]From Lee and Foley (2008).
[2] Dose to MEI at SRS Boundary = Peak Flux × SRS Boundary Dose Release Factor.
[3]Disposal Limit = 10 mrem/yr / Dose to MEI at SRS Boundary per Year per Ci

Table 18. Peak Fluxes, Time to Peak Fluxes, 100 m Boundary Dose Release Factors, and 100 m Boundary Dose to the MEI for ARP/MCU Saltstone in Vault 1

Radionuclide	Peak Flux ($Ci/m^2/yr$) /Ci/m^2)	Time to Peak Flux (yrs)	100 m Boundary Dose Release Factor[1] (mrem/Ci)	Dose to MEI at 100 m Boundary[2] (mrem/yr/Ci)
^{14}C	4.18E-14	136.0	3.7E-03	1.5E-16
^{36}Cl	2.07E-27	283.1	7.9E-03	1.6E-29
^{129}I	9.02E-31	715.8	5.5E+00	5.0E-30
^{125}Sb	3.51E-46	4.4	1.1E-01	3.9E-47
^{79}Se	4.14E-16	291.7	1.1E-02	4.6E-18
^{126}Sn	1.64E-70	350.8	4.9E+00	8.1E-70
$^{3}H_2$	3.12E-13	9.7	7.7E-05	2.4E-17
^{99}Tc	2.72E-77	311.2	2.9E-02	7.9E-79

[1]From Lee and Foley (2008).
[2] Dose to MEI at 100 m Boundary = Peak Flux × 100 m Boundary Dose Release Factor.
[3]Disposal Limit = 10 mrem/yr / Dose to MEI at 100 m Boundary per Year per Ci

Table 19. Peak Fluxes, Time to Peak Fluxes, SRS Boundary Dose Release Factors, and SRS Boundary Dose to the MEI for SWPF Saltstone in Vault 2 (and future disposal units)

Radionuclide	Peak Flux ($Ci/m^2/yr$) /Ci/m^2)	Time to Peak Flux (yrs)	SRS Boundary Dose Release Factor[1] (mrem/Ci)	Dose to MEI at SRS Boundary[2] (mrem/yr/Ci)
^{14}C	4.27E-14	147.3	1.1E-04	4.7E-18
^{36}Cl	2.12E-27	305.1	3.6E-04	7.7E-31
^{129}I	9.22E-31	787.0	4.8E-02	4.4E-32
^{125}Sb	2.10E-46	6.1	6.6E-03	1.4E-48
^{79}Se	4.24E-16	317.5	6.0E-04	2.6E-19
^{126}Sn	1.68E-70	379.9	3.0E-01	5.1E-71
$^{3}H_2$	2.97E-13	10.4	2.3E-06	6.7E-19
^{99}Tc	2.77E-77	337.1	1.8E-03	5.0E-80

[1]From Lee and Foley (2008).
[2] Dose to MEI at SRS Boundary = Peak Flux × SRS Boundary Dose Release Factor.
[3]Disposal Limit = 10 mrem/yr / Dose to MEI at SRS Boundary per Year per Ci

Table 20. Peak Fluxes, Time to Peak Fluxes, 100 m Boundary Dose Release Factors, and 100 m Boundary Dose to the MEI for SWPF Saltstone in Vault 2 (and future disposal units)

Radionuclide	Peak Flux ($Ci/m^2/yr$) /Ci/m^2)	Time to Peak Flux (yrs)	100 m Boundary Dose Release Factor[1] (mrem/Ci)	Dose to MEI at 100 m Boundary[2] (mrem/yr/Ci)
^{14}C	4.27E-14	147.3	3.7E-03	1.6E-16
^{36}Cl	2.12E-27	305.1	7.9E-03	1.7E-29
^{129}I	9.22E-31	787.0	5.5E+00	5.1E-30
^{125}Sb	2.10E-46	6.1	1.1E-01	2.3E-47
^{79}Se	4.24E-16	317.5	1.1E-02	4.7E-18
^{126}Sn	1.68E-70	379.9	4.9E+00	8.2E-70
$^{3}H_2$	2.97E-13	10.4	7.7E-05	2.3E-17
^{99}Tc	2.77E-77	337.1	2.9E-02	8.0E-79

[1]From Lee and Foley (2008).
[2] Dose to MEI at 100 m Boundary = Peak Flux × 100 m Boundary Dose Release Factor.
[3]Disposal Limit = 10 mrem/yr / Dose to MEI at 100 m Boundary per Year per Ci

Table 21. Peak Fluxes, Time to Peak Fluxes, SRS Boundary Dose Release Factors, and SRS Boundary Dose to the MEI for DDA Saltstone in Vault 4

Radionuclide	Peak Flux ($Ci/m^2/yr$) /Ci/m^2)	Time to Peak Flux (yrs)	SRS Boundary Dose Release Factor[1] (mrem/Ci)	Dose to MEI at SRS Boundary[2] (mrem/yr/Ci)
^{14}C	7.24E-14	141.5	1.1E-04	7.9E-18
^{36}Cl	3.59E-27	291.7	3.6E-04	1.3E-30
^{129}I	1.56E-30	787.0	4.8E-02	7.4E-32
^{125}Sb	5.07E-46	5.0	6.6E-03	3.3E-48
^{79}Se	7.18E-16	303.6	6.0E-04	4.3E-19
^{126}Sn	2.84E-70	363.3	3.0E-01	8.6E-71
$^{3}H_2$	5.23E-13	10.0	2.3E-06	1.2E-18
^{99}Tc	4.69E-77	323.9	1.8E-03	8.4E-80

[1]From Lee and Foley (2008).
[2] Dose to MEI at SRS Boundary = Peak Flux × SRS Boundary Dose Release Factor.
[3]Disposal Limit = 10 mrem/yr / Dose to MEI at SRS Boundary per Year per Ci

Table 22. Peak Fluxes, Time to Peak Fluxes, 100 m Boundary Dose Release Factors, and 100 m Boundary Dose to the MEI for DDA Saltstone in Vault 4

Radionuclide	Peak Flux ($Ci/m^2/yr$) /Ci/m^2)	Time to Peak Flux (yrs)	100 m Boundary Dose Release Factor[1] (mrem/Ci)	Dose to MEI at 100 m Boundary[2] (mrem/yr/Ci)
^{14}C	7.24E-14	141.5	3.7E-03	2.7E-16
^{36}Cl	3.59E-27	291.7	7.9E-03	2.8E-29
^{129}I	1.56E-30	787.0	5.5E+00	8.6E-30
^{125}Sb	5.07E-46	5.0	1.1E-01	5.6E-47
^{79}Se	7.18E-16	303.6	1.1E-02	7.9E-18
^{126}Sn	2.84E-70	363.3	4.9E+00	1.4E-69
$^{3}H_2$	5.23E-13	10.0	7.7E-05	4.0E-17
^{99}Tc	4.69E-77	323.9	2.9E-02	1.4E-78

[1]From Lee and Foley (2008).
[2] Dose to MEI at 100 m Boundary = Peak Flux × 100 m Boundary Dose Release Factor.
[3]Disposal Limit = 10 mrem/yr / Dose to MEI at 100 m Boundary per Year per Ci

Table 23. Peak Fluxes, Time to Peak Fluxes, SRS Boundary Dose Release Factors, and SRS Boundary Dose to the MEI for ARP/MCU Saltstone in Vault 4

Radionuclide	Peak Flux ($Ci/m^2/yr$) /Ci/m^2)	Time to Peak Flux (yrs)	SRS Boundary Dose Release Factor[1] (mrem/Ci)	Dose to MEI at SRS Boundary[2] (mrem/yr/Ci)
^{14}C	4.10E-15	152.5	1.1E-04	4.5E-19
^{36}Cl	2.04E-28	315.9	3.6E-04	7.4E-32
^{129}I	8.86E-32	819.0	4.8E-02	4.2E-33
^{125}Sb	1.84E-47	6.2	6.6E-03	1.2E-49
^{79}Se	4.08E-17	328.8	6.0E-04	2.5E-20
^{126}Sn	1.61E-71	391.5	3.0E-01	4.9E-72
$^{3}H_2$	2.79E-14	10.6	2.3E-06	6.3E-20
^{99}Tc	2.66E-78	350.8	1.8E-03	4.8E-81

[1]From Lee and Foley (2008).
[2] Dose to MEI at SRS Boundary = Peak Flux × SSRS Boundary Dose Release Factor.
[3]Disposal Limit = 10 mrem/yr / Dose to MEI at SRS Boundary per Year per Ci

Table 24. Peak Fluxes, Time to Peak Fluxes, 100 m Boundary Dose Release Factors, and 100 m Boundary Dose to the MEI for ARP/MCU Saltstone in Vault 4

Radionuclide	Peak Flux ($Ci/m^2/yr$) /Ci/m^2)	Time to Peak Flux (yrs)	100 m Boundary Dose Release Factor[1] (mrem/Ci)	Dose to MEI at 100 m Boundary[2] (mrem/yr/Ci)
^{14}C	4.10E-15	152.5	3.7E-03	1.5E-17
^{36}Cl	2.04E-28	315.9	7.9E-03	1.6E-30
^{129}I	8.86E-32	819.0	5.5E+00	4.9E-31
^{125}Sb	1.84E-47	6.2	1.1E-01	2.0E-48
^{79}Se	4.08E-17	328.8	1.1E-02	4.5E-19
^{126}Sn	1.61E-71	391.5	4.9E+00	7.9E-71
$^{3}H_2$	2.79E-14	10.6	7.7E-05	2.1E-18
^{99}Tc	2.66E-78	350.8	2.9E-02	7.7E-80

[1]From Lee and Foley (2008).
[2] Dose to MEI at 100 m Boundary = Peak Flux × 100 m Boundary Dose Release Factor.
[3]Disposal Limit = 10 mrem/yr / Dose to MEI at 100 m Boundary per Year per Ci

Table 25. Simulated Peak Instantaneous Rn-222 Flux over 10,000-Years at the Land Surface for Vault 1 DDA Saltstone

Parent Source (1 Ci/m^2)	**Peak Instantaneous Rn-222 flux at Land Surface (pCi/m^2/sec) / (Ci/m^2)**
Pu-238	3.39E-14
U-238	1.15E-12
U-234	9.65E-11
Th-230	1.31E-09
Ra-226	1.43E-09

Table 26. Simulated Peak Instantaneous Rn-222 Flux over 10,000-Years at the Land Surface for Vault 1 ARP/MCU Saltstone

Parent Source (1 Ci/m^2)	**Peak Instantaneous Rn-222 flux at Land Surface (pCi/m^2/sec) / (Ci/m^2)**
Pu-238	3.15E-14
U-238	1.07E-12
U-234	8.96E-11
Th-230	1.22E-09
Ra-226	1.33E-09

Table 27. Simulated Peak Instantaneous Rn-222 Flux over 10,000-Years at the Land Surface for Vault 2 (and future disposal units) SWPF Saltstone

Parent Source (1 Ci/m^2)	**Peak Instantaneous Rn-222 flux at Land Surface (pCi/m^2/sec) / (Ci/m^2)**
Pu-238	1.63E-20
U-238	5.55E-19
U-234	4.64E-17
Th-230	6.31E-16
Ra-226	6.86E-16

Table 28. Simulated Peak Instantaneous Rn-222 Flux over 10,000-Years at the Land Surface for Vault 4 DDA Saltstone

Parent Source ($1\ Ci/m^2$)	**Peak Instantaneous Rn-222 flux at Land Surface ($pCi/m^2/sec$) / (Ci/m^2)**
Pu-238	1.41E-16
U-238	4.79E-15
U-234	4.00E-13
Th-230	5.45E-12
Ra-226	5.92E-12

Table 29. Simulated Peak Instantaneous Rn-222 Flux over 10,000-Years at the Land Surface for Vault 4 ARP/MCU Saltstone

Parent Source ($1\ Ci/m^2$)	**Peak Instantaneous Rn-222 flux at Land Surface ($pCi/m^2/sec$) / (Ci/m^2)**
Pu-238	1.28E-16
U-238	4.35E-15
U-234	3.64E-13
Th-230	4.96E-12
Ra-226	5.39E-12

Distribution

J. J. Mayer, 773-42A
R. S. Aylward, 773-42A
H. H. Burns, 999-W
D. A. Crowley, 773-43A
J. C. Griffin, 773-A
K. L. Dixon, 773-42A
M. A. Phifer, 773-42A
E. L. Wilhite, 773-43A
M. B. Birk, 766-H
J. L. Newman, 766-H
M. H. Layton, 766-H
K. H. Rosenberger, 766-H
T. C. Robinson, 766-H
E&CPT Files 773-43A, Rm. 213

APPENDIX A. DEVELOPMENT OF LIQUID TO GAS PARTITIONING COEFFICIENTS FOR THE AIR PATHWAY ANALYSIS

The ideal gas law is used to develop a relationship between partial pressure and the concentration of contaminant in the gas phase.

$$PV = nRT \tag{1}$$

where:
P = pressure, atm
V = volume, m^3
n = number moles
R = Universal Gas Constant, 8.3143 J/mol-K
T = temperature, K

Rearranging equation 1 yields the volumetric concentration of contaminant in the gas phase.

$$\frac{n}{V} = \frac{P}{RT} \tag{2}$$

$$c_g^v = \frac{n}{V} \tag{3}$$

where:
c_g^v = volumetric concentration of contaminant in the gas phase, mol/ml .

Making the assumption of a single ideal gas occupying the representative volume, the pressure term, P, can be thought of as the partial pressure

$$c_g^v = \frac{X_p}{RT} \tag{4}$$

where:
X_p = partial pressure of the gas, atm

Rearranging and solving for the partial pressure yields:

$$X_p = c_g^v RT \tag{5}$$

Henry's law may be written as:

$$[X_a] = H\, X_p \tag{6}$$

where:

X_a = aqueous concentration of contaminant on a mass basis, mol/g
X_p = partial pressure of the gas, atm
H = Henry's law constant, mol/atm-g

The partitioning coefficient, K_d, may be defined as:

$$K_d = \frac{c_f^m}{c_g^v} \tag{7}$$

where
c_f^m = aqueous concentration of contaminant on a mass basis, mol/g

By analogy,

$$c_f^m = X_a \tag{8}$$

Substituting equation 8 into equation 6 yields:

$$c_f^m = H\, X_p \tag{9}$$

Substituting equation 5 into equation 9 yields:

$$c_f^m = H\, c_g^v RT \tag{10}$$

Rearranging and grouping terms in equation 10 yields:

$$c_f^m = (H\, RT) c_g^v \tag{11}$$

By analogy with equation 7,

$$K_d = (H\, RT) \tag{12}$$

Example Calculation:

For C-14, from Table 10, H = 1.4 x 10^4 mol/atm-kg

$$K_d = (H\ R\ T)$$

$$K_d \frac{ml}{g} = \left(1.4\,x10^4 \frac{mol}{atm-kg}\right)\left(8.3143 \frac{J}{mol-K}\right)(293\,K)\left(\frac{atm-m^2}{101325\,N}\right)\left(\frac{N-m}{J}\right)\left(10^6 \frac{ml}{m^3}\right)\left(\frac{kg}{1000\,g}\right)$$

$$K_d = 1.4\,x10^4 \frac{(8.3143)(293)(10^6)}{(101325)(10^3)} \frac{ml}{g}$$

$$K_d = 3.37\,x10^5 \frac{ml}{g}$$

APPENDIX B. DESIGN CHECK

Tad Whiteside/SRNL/Srs
12/17/2008 01:03 PM

To Kenneth Dixon/SRNL/Srs@srs
cc Mark Phifer/SRNL/Srs@Srs
bcc
Subject Re: Design Check

That takes care of the only issues I had.

Tad

Tad Whiteside, PhD
Senior Scientist
Savannah River National Lab
803-725-8267
tad.whiteside@srnl.doe.gov
Kenneth Dixon/SRNL/Srs

Kenneth Dixon/SRNL/Srs
12/17/2008 12:16 PM

To Tad Whiteside/SRNL/Srs@Srs
cc Mark Phifer/SRNL/Srs@srs
Subject Re: Design Check

Tad,

I confirmed the error in the spreadsheet is a typo and corrected it. The model grid is correct. Also, I corrected the units as noted in the flux_rn.xls spreadsheets.

If this satisfies your comments, please respond back as such and we will consider the design check complete.

Thanks for your quick response and thorough check.

Ken
5-5205

Tad Whiteside/SRNL/Srs

Tad Whiteside/SRNL/Srs
12/17/2008 08:02 AM

To Kenneth Dixon/SRNL/Srs@srs
cc Mark Phifer/SRNL/Srs@Srs
Subject Re: Design Check

My comments are below:

Kenneth Dixon/SRNL/Srs

Please perform a design check of the document SRNL-STI-2008-00447_Rev06.doc and associated files. We have modified the original analysis to incorporate liquid-gas partitioning of radionuclides in the air pathway analysis. Also, we eliminated the assumption that the waste layer is dry. Saturation values for the waste layer and grout cap were obtained from the SDF PA vadose zone model. This report covers the air and radon pathway analysis conducted for the Saltstone Disposal Facility. The files to be checked may be located at the following path:

\\wg02\KLD\Salt_Air_Radon_DesignCheck

This analysis included 5 cases which are:

1)Vault 1 with DDA saltstone
2)Vault 1 with MCU saltstone
3)Vault 2 with SWPF saltstone
4)Vault 4 with DDA saltstone
5)Vault 4 with MCU saltstone

The file structure implemented is consistent with this nomenclature. We meet to discuss the general concepts and file layout so that you can get up to speed quicker if you would like to do so. The cose code for your time is WCZPAREV2.

Thanks,
Ken
5-5205

Design checking should include the following elements:

- Verify that the approach used to implement liquid-gas partitioning for the air pathway analysis is sound. This is discussed in Section 3.2 and Appendix A.
  This approach seems reasonable

- Check the PORFLOW input, output, and associated graphics files to ensure that the conceptual approach has been correctly implemented as outlined in SRNL-STI-2008-00447_Rev06.doc.
  The approach has been implemented correctly

- Check the worksheets within salt_model_setup.xls for accuracy. Values may be spot checked.
  The Vault_1 table in the *.xls file and Table1 in the document do not match on the "Saltstone (DDA or ARP/MCU)" row - in the *.xls it is listed as 240, in the document it is presented as 288 (which I believe is the correct value based on figure 3).

- Check the worksheets within Salt_DiffusionCoefficients.xls for accuracy. Values may be spot checked.
  They are accurate.

- Check that the grid dimensions used in the PORFLOW models adequately represent the dimensions of Vault 1, Vault 2, and Vault 4, and cover material. Check that the grid density is adequate to compute diffusive flux of radon at the land surface.
  They seem to be reasonable. I believe that the density is adequate.

- Verify that the results of the PORFLOW simulation given in \<vault>\<parent>\flux.out are reasonable and that these results have been accurately transferred to file \flux_rn.xls for each parent radionuclide, vault, and waste configuration.
  They are reasonable and have been transferred correctly.

- Check that the flux summaries given in file \<vault>\flux_rn.xls, worksheet "Summary" are accurate and that these data have been accurately presented in SRNL-STI-2008-00447_Rev06.doc.
The data has been accurately presented although the units label on column 2 of tables 25-27 does not match up: In those columns it is: (pCi/m2/sec)/(Ci/m2) in the worksheet it is: (pCi/m2/sec)

- Check that the flux curves (radon and air pathway) presented in SRNL-STI-2008-00447_Rev06.doc are reasonable.
They look reasonable - matching up with the data.

- Confirm that the correct diffusion coefficients are used for each radionuclide in the PORFLOW input file \air\run.dat. These values may be spot checked.
The correct diff. coefficients are used.

- Verify that the results of the PORFLOW simulation given in \<vault>\air\flux.out are reasonable and that these results have been accurately transferred to file \<vault>\air\LimitsCalc.xls, worksheet "Porflow_Flux".
They are reasonable.

- Verify that the dose calculations are accurate in \<vault>\air\LimitsCalc.xls, worksheet "<vault>" and verify that these data have been accurately presented in SRNL-STI-2008-00447_Rev06.doc.
They are accurate.

- Verify that the appropriate dose release factors are used in the disposal limit calculations presented in \<vault>\air\LimitsCalc.xls, worksheet "<vault>".
They are the appropriate factors

- Check that the flux summary data from file \<vault>\air\LimitsCalc.xls, worksheet "Porflow_Flux" have been accurately presented in SRNL-STI-2008-00447_Rev06.doc. These values may be spot checked.
They are accurate and have been accurately presented in the document.